

HUMBOLDT-UNIVERSITÄT ZU BERLIN



LEBENSWISSENSCHAFTLICHE FAKULTÄT
INSTITUT FÜR BIOLOGIE

BACHELORARBEIT

ZUM ERWERB DES AKADEMISCHEN GRADES
BACHELOR OF SCIENCE

A Physiologically Based Model of Indocyanine Green
Liver Function Tests - Effects of Physiological Factors,
Hepatic Disease and Hepatic Surgery

Ein physiologisch-basiertes Modell der Indocyaningrün
Leberfunktionstests - Effekte von physiologischen
Faktoren, Lebererkrankung und Leberchirurgie

vorgelegt von

Adrian Köller

Matrikelnummer: 589704

E-Mail: adrian.koeller@arcor.de

Geburtsdatum und -ort: 26.11.1999 Pforzheim

angefertigt in der Arbeitsgruppe Systems Medicine of the Liver

am Institut für Theoretische Biologie

Berlin, im März 2021

Erstprüfer: **Dr. Matthias König**

Zweitprüfer: **Prof. Dr. Hanspeter Herzel**

Contents

1	Introduction	5
1.1	Indocyanine green (ICG)	5
1.2	Pharmacokinetics	6
1.3	ICG pharmacokinetic parameters	7
1.4	Blood flow	8
1.5	Plasma proteins	8
1.6	Disease	10
1.6.1	Cirrhosis	10
1.7	Liver surgery (hepatectomy)	11
1.8	Physiological-based pharmacokinetic model (PBPK)	12
1.9	Question, scope and hypotheses	12
2	Methods	14
2.1	ICG pharmacokinetics parameters	14
2.2	ICG data	15
2.2.1	Data curation	15
2.3	Physiological-based pharmacokinetics models (PBPK)	16
2.4	Parameter fitting	16
2.5	Uncertainty analysis	17
2.6	Sensitivity analysis	17
3	Results	18
3.1	ICG data	18
3.2	Computational model of ICG	21
3.2.1	Physiological based pharmacokinetics model (PBPK)	21
3.2.2	Distribution	21
3.2.3	Blood flow	22
3.2.4	Hepatic metabolism and biliary excretion	23
3.2.5	Plasma proteins (bilirubin)	24
3.2.6	Liver disease (cirrhosis)	25
3.2.7	Liver surgery (hepatectomy)	26
3.3	Parameter fitting	26
3.4	Model performance	30
3.4.1	Reference simulation	30
3.4.2	ICG timecourses	33
3.4.3	Dose dependency	36
3.5	Model application	37
3.5.1	Disease (cirrhosis)	37
3.5.2	Blood flow dependency	44
3.5.3	Plasma proteins (bilirubin dependency)	49
3.5.4	Hepatectomy	51
3.6	Sensitivity analysis	56
3.6.1	Protein dependency	58
4	Discussion	60
4.1	Data	60
4.2	Physiological-based modeling	60
4.3	Bilirubin	61
4.4	Blood flow	62
4.5	Hepatectomy	62
4.6	Disease	63
5	Outlook	64

6	Supplement	66
6.1	Dose dependency	66
6.2	Model	67

Abstract

English

The evaluation of hepatic function and functional capacity are essential tasks in hepatology. Indocyanine Green (ICG) is a widely applied test compound that is used in clinical routine to evaluate hepatic function.

Accurate assessment of liver-function through ICG pharmacokinetics is challenging because the elimination of ICG is influenced by physiological factors such as liver perfusion as well as the health status of the patient. Important questions for the functional evaluation are how blood flow, plasma protein binding or surgical interventions can influence the distribution and elimination of ICG. In the course of this project, these questions were studied by the means of computational modeling to evaluate ICG dynamics *in silico*.

Within this work a physiological-based model of ICG pharmacokinetics was developed. For the parameterization and validation of the model a database of ICG pharmacokinetic data was established. The model was applied to study (i) the effect of liver disease, specifically liver cirrhosis, on ICG pharmacokinetics; (ii) how hepatic blood flow and other cardiovascular parameters affect ICG-elimination; and (iii) the role of plasma protein binding of ICG and its impact on ICG pharmacokinetics. Finally, the model was applied to analyse the effect of liver resection (hepatectomy) on ICG-elimination and the value of ICG as a predictive measure for postoperative outcome.

The model is able to accurately predict changes in ICG pharmacokinetics caused by changes in blood flow and plasma proteins as well as liver cirrhosis. Furthermore, the model is able to accurately predict postoperative changes of ICG-elimination after liver resection, showing its potential value as a clinical tool.

German

Die Beurteilung der Leberfunktion und der funktionellen Kapazität sind essenzielle Aufgaben in der Hepatologie. Indocyaningrün (ICG) ist eine weit verbreitete Testsubstanz, die in der klinischen Routine zur Beurteilung der Leberfunktion eingesetzt wird.

Die akkurate Beurteilung der Leberfunktion durch die ICG-Pharmakokinetik stellt eine Herausforderung dar, da die Elimination von ICG von physiologischen Faktoren wie der Leberperfusion sowie dem Gesundheitszustand des Patienten beeinflusst wird. Wichtige Fragen für die Funktionsbewertung sind, wie Blutfluss, Plasmaproteinbindung oder chirurgische Eingriffe die Verteilung und Elimination von ICG beeinflussen können. Im Rahmen dieses Projektes wurden diese Fragen mittels computergestützter Modellierung zur Bewertung der ICG-Dynamik *in silico* untersucht.

Im Rahmen dieser Arbeit wurde ein physiologisch basiertes Modell der ICG-Pharmakokinetik entwickelt. Für die Parametrisierung und Validierung des Modells wurde eine Datenbank mit ICG pharmakokinetischen Daten erstellt. Das Modell wurde angewandt, um (i) die Auswirkung von Lebererkrankungen, insbesondere von Leberzirrhose, auf die ICG-Pharmakokinetik zu untersuchen; (ii) zu untersuchen wie der hepatische Blutfluss und andere kardiovaskuläre Parameter die ICG-Eliminierung beeinflussen; und (iii) die Rolle der Plasmapro-

teinbindung von ICG und deren Einfluss auf die ICG-Pharmakokinetik zu untersuchen. Schließlich wurde das Modell angewandt, um den Effekt einer Leberresektion (Hepatektomie) auf die ICG-Elimination und den Wert von ICG als Vorhersagemaßstab für das postoperative Ergebnis zu analysieren.

Das Modell ist in der Lage, Veränderungen in der ICG-Pharmakokinetik, die durch Variationen des Blutflusses und der Plasmaproteine sowie durch eine Leberzirrhose verursacht werden, genau vorherzusagen. Darüber hinaus ist das Modell in der Lage, postoperative Veränderungen der ICG-Elimination nach einer Leberresektion genau vorherzusagen, was seinen potenziellen Wert als klinisches Hilfsmittel aufzeigt.

1 Introduction

Accurate evaluation of hepatic function and the functional capacity of the liver are important tasks in hepatology. An important method to determine liver function is to apply a test compound which is specifically cleared by the liver using the time course of plasma disappearance of the substance to estimate liver function. Indocyanine green (ICG) is a widely applied test compound that is used in clinical routine to evaluate hepatic function, e.g., to estimate the functional reserve in hepatectomy. Accurate assessment of liver-function via ICG is challenging because the elimination of ICG can be influenced by confounding factors such as liver perfusion, plasma proteins, or health status of the patient. An important question for the functional evaluation is therefore how these factors can influence the ICG parameters used for patient evaluation.

In this project, this question was studied by the means of computational modeling.

1.1 Indocyanine green (ICG)

Indocyanine green (IUPAC name: sodium 4-[2-[(1E,3E,5E,7Z)-7-[1,1-dimethyl-3-(4-sulfonatobutyl)benzo[e]indol-2-ylidene]hepta-1,3,5-trienyl]-1,1-dimethylbenzo[e]indol-3-iun-3-yl]butane-1-sulfonate) is an inert, anionic, water-soluble, tri-carbocyanine dye (see Fig. 1) that has been used as a test-substance to assess hepatic function since the 1950s.

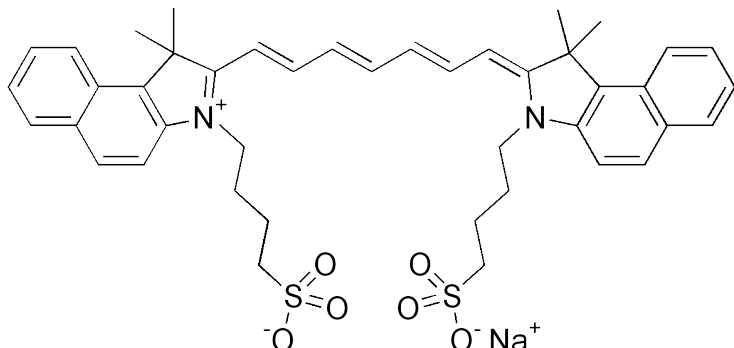


Figure 1: Structure of indocyanine green; CHEBI:31696; inchikey: MOFVSTNWEDAEEK-UHFFFAOYSA-M

ICG is eliminated exclusively by the liver and excreted unchanged into the bile [8]. ICG is not reabsorbed by the intestine and therefore does not undergo enterohepatic circulation [75]. These properties of ICG make it an ideal test substance, because changes in plasma concentration reflect uptake by the liver and excretion in the bile.

To test liver function ICG is typically applied as an intravenous bolus injection of around 0.5-5 mg/kg and multiple blood samples are taken from shortly after the administration until around 30 min after application (see Fig. 2)

Since ICG was first described as a test substance for liver function tests, there has been a development towards measuring ICG pharmacokinetics non-invasively. A non-invasive procedure was first described in 1967 by Leevy

et al. using ear densitometry [41]. With the development of the LiMON-technology (<https://www.getinge.com/de/produktkatalog/limon-technologie/>), a bed-side monitoring device, ICG pharmacokinetics can be measured non-invasively, which has lead to an increase in clinical use in recent years [43]. The value of non-invasive procedures as opposed to invasive measurements has been assessed extensively [58, 14, 42].

1.2 Pharmacokinetics

After an intravenous bolus administration, the ICG-elimination curve follows a standard indicator dilution curve (see Fig. 2). The concentration reaches its peak shortly after the injection. Afterwards it declines as ICG is eliminated from the plasma by the liver and excreted into the bile. ICG elimination is slower in a cirrhotic patient because liver function is impaired as described in Sec. 1.6.1.

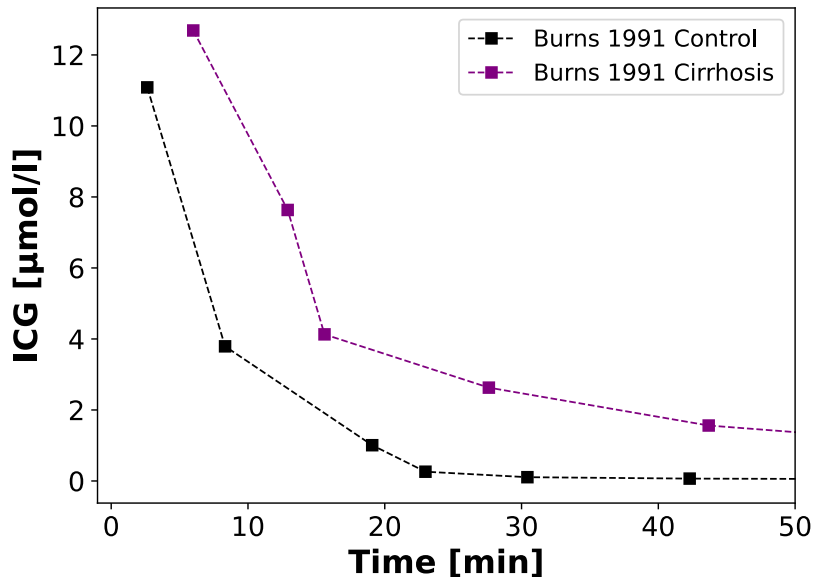


Figure 2: Example of an ICG pharmacokinetic time course in a healthy and a cirrhotic subject after a bolus injection of 0.5 mg/kg ICG. The data was published by Burns et al. [6].

The hepatic clearance of a drug is determined by the extraction-ratio of the drug ER and the hepatic blood flow Q_h .

$$CL_h = ER \cdot Q_h \quad (1)$$

The extraction-ratio describes the fraction of the substance that is cleared from the blood in one passage through the liver. It is calculated as follows:

$$ER = \frac{C_{ar} - C_{hv}}{C_{hv}} \quad (2)$$

where C_{ar} is the ICG concentration in the arterial plasma and C_{hv} is the ICG concentration in the hepatic venous plasma.

Based on simple compartment models of drug clearance three physiological factors are relevant for the hepatic extraction-ratio of a drug. First, the intrinsic clearance of the drug CL_{int} is a parameter that represents the metabolizing enzyme activity. Second, the unbound fraction of drug in the blood f_u , because generally only unbound drug is taken up by the liver. And third, the hepatic blood flow Q_h :

$$ER = \frac{f_u \cdot CL_{int}}{Q_h + f_u \cdot CL_{int}} \quad (3)$$

Hepatic clearance results as:

$$CL_h = Q_h \cdot \frac{f_u \cdot CL_{int}}{Q_h + f_u \cdot CL_{int}} \quad (4)$$

However, the influence of these factors on the hepatic clearance vary, depending on f_u and CL_{int} . When f_u and CL_{int} are very low compared to hepatic blood flow (low extraction-ratio; $f_u \cdot CL_{int} \ll Q_h$), hepatic clearance can be approximated as

$$CL_h = f_u \cdot CL_{int} \quad (5)$$

and is therefore independent of the hepatic blood flow. In return, when f_u and CL_{int} are high (high extraction-ratio, $f_u \cdot CL_{int} \gg Q_h$), hepatic clearance can be approximated as

$$CL_h = Q_h \quad (6)$$

and therefore only depends on hepatic blood flow [4]. The extraction-ratio of ICG in healthy human subjects is 0.6 - 0.9 [18, 16, 40]. Therefore a strong dependency on blood flow and less dependency on protein binding and enzyme activity of ICG-clearance is expected.

1.3 ICG pharmacokinetic parameters

Hepatic function based on ICG is quantified using various measurements calculated on the timecourse of ICG in plasma (see Tab. 1) [60].

Table 1: Pharmacokinetic parameters used in the evaluation of liver function based on ICG pharmacokinetics

Variable	Description	Unit
ICG-PDR	ICG Plasma Disappearance-Rate	%/min
ICG-R15	ICG Retention-Rate at 15 min	%
CL_{ICG}	ICG-clearance	ml/min
$ICG-t_{1/2}$	ICG half-life time	min

ICG-PDR and ICG-R15 are used in a clinical context to evaluate liver function. Both of them are used as a predictive measure of liver surgery outcome. Haegele et al. [22] were able to show that reduced ICG-PDR and increased ICG-R15 significantly predict postoperative liver dysfunction. Hemming et al. [24]

showed that in contrast to other parameters ICG-clearance successfully predicted post-operative mortality in cirrhotic patients undergoing hepatic resection.

However, these ICG parameters have their limitations as many factors like blood flow, protein binding or disease affect ICG elimination.

1.4 Blood flow

As described in Sec. 1.2, due to the high extraction-ratio ICG-elimination depends strongly on hepatic blood flow. The effect of varying hepatic blood flow on ICG-elimination has been studied in many instances.

Gadano et al. [16] and Huet and Villeneuve [28] studied the relationship between hepatic blood flow and ICG-clearance in cirrhosis and in control subjects. Both found good positive correlation in healthy subjects but poor correlation in cirrhosis. Kanstrup and Winkler [31] found good positive correlation between hepatic blood flow and ICG-clearance, by changing hepatic blood flow pharmacologically or by food ingestion. Rowell et al. [59] studied the changes in hepatic blood flow and ICG-clearance during exercise. Huet and Lelorier [27] studied the effects of smoking and chronic hepatitis B on ICG-kinetics reporting hepatic blood flow alongside ICG pharmacokinetics.

Due to the dependency of ICG on blood flow, ICG has been used to estimate hepatic blood flow using the Fick principle [40]. By administering an intravenous infusion of ICG below the liver's removal capacity, a steady state ICG concentration is reached after one hour. By measuring hepatic venous and peripheral arterial concentrations, hepatic blood flow can be calculated as

$$Q_h = \frac{R}{C_{ar} - C_{hv}} \quad (7)$$

where R is the infusion rate in mg/min, C_{ar} is the concentration of ICG in arterial blood and C_{hv} is the concentration of ICG in hepatic venous blood.

However, this method of measuring hepatic blood flow requires hepatic venous catheterization which is highly invasive. A less-invasive method of estimating hepatic blood flow through ICG-concentration measurements was developed in 1983 by Grainger et al. [18].

Hepatic blood flow itself is influenced by many different variables like blood pressure, portal resistance or cardiac output. Hepatic blood flow is often altered in disease or after liver surgery (e.g. hepatectomy). Due to the dependency of ICG measurements on liver perfusion, haemodynamic stability is required during ICG evaluations. Accurate estimation of liver function via ICG pharmacokinetics can become challenging in disease which alters systemic circulation or hepatic circulation. A better understanding of the effects of blood flow on ICG elimination would be important for a more accurate evaluation of ICG liver function tests.

1.5 Plasma proteins

When ICG enters the bloodstream, it is bound to plasma-proteins (serum albumin and lipoproteins). An equilibrium between plasma bound ICG and free ICG exists, that can influence the elimination of ICG. However, no consensus on the protein-binding of ICG or its mechanism let alone its effect on ICG elimination

exists in the literature. The main complicating issues are that ICG binds to a number of different plasma proteins and the extend to which it binds to each depends on the concentration of ICG itself as well as the concentration of the protein [54].

In 1960 Cherrik et al. [9] reported that 95% of ICG binds to albumin. Later research suggested that the protein-binding of ICG depends on its concentration in plasma. At ICG concentrations typically observed in the context of a liver function tests, ICG binds mainly to lipoproteins [30]. If ICG-concentration in plasma exceeds $50 \mu\text{mol/l}$ the binding shifts towards albumin [54]. In addition to that, Kamisaka et al. [30] reported evidence that the binding of ICG to plasma proteins can change in various liver diseases.

The effect of increasing albumin concentrations on ICG-elimination was studied by Keiding et al. [35] reporting an increase in ICG-elimination when albumin concentrations were increased. This opposes the traditional idea that a decrease in the free-fraction of a protein bound drug reduces its elimination. Instead, some studies suggest a protein mediated uptake mechanism of ICG [3, 63]. In 1966 Baker and Bradley [2] suggested that the binding-proteins could play a role in hepatic uptake of organic anions such as ICG or BSP (bromosulphalein). How exactly this works and what membrane-proteins are involved requires further research. In summary there is no clear picture on the protein binding of ICG and how this affects ICG uptake.

In contrast much more information exists on the alteration of ICG elimination due to bilirubin. Bilirubin is a fundamental end product of heme degradation. It exists primarily in blood, and is bound almost completely to albumin. Naturally, ICG and bilirubin compete for albumin binding-sites. Assuming that ICG can only be taken up by the liver through a protein-mediated uptake mechanism, bilirubin will competitively inhibit ICG uptake. Higher plasma concentrations of bilirubin therefore lead to a decrease in ICG-elimination [55, 5].

Because bilirubin plasma concentrations are itself used to evaluate liver function (e.g. in Child-Pugh-Turcotte-Score) it is often reported alongside ICG pharmacokinetic parameters in clinical studies. Martin et al. [45] found a significant reduction of ICG-elimination in Gilbert's disease, which affects the livers ability to process bilirubin and therefore leads to higher plasma levels. Branch et al. [5] and Kawasaki et al. [32] compared the ICG-clearance of healthy subjects with cirrhotic patients and found good correlation of bilirubin concentration and ICG-clearance as bilirubin levels are increased in cirrhosis. Caesar et al. [8] found similar results regarding the extraction-ratio of ICG as well as its elimination rate constant (ICG-kel). D'Onofrio et al. [13] reported bilirubin plasma concentrations alongside ICG pharmacokinetics in different liver diseases, e.g. chronic hepatitis B and C, hepatocellular carcinoma as well as peripheral and hilar cholangiocarcinoma showing a significantly reduced ICG-elimination when bilirubin levels were increased.

Within this work we specifically looked at the inhibitory effect of bilirubin on ICG elimination presumably mediated via plasma proteins. Because bilirubin plasma concentrations vary greatly in disease - especially liver disease - the bilirubin effect is a good example for studying the influence of plasma proteins on ICG-elimination.

1.6 Disease

In general, liver disease is accompanied with a loss of liver function especially advanced and more severe liver disease. However, the reduction in liver function can itself have different causes and often goes unnoticed until the disease has reached an advanced stage.

The effects of liver disease on ICG-elimination have been studied extensively. The effect of different stages of primary biliary cholangitis (PBC) on ICG pharmacokinetics was described by Vaubourdolle et al. [72]. Gilbert's disease was found to reduce ICG-elimination as described by Martin et al. [45]. Gadano et al.[16] found that ICG-clearance is reduced in patients with hepatic fibrosis as well as cirrhosis. Huet et al. [27] however found no significant difference in ICG-clearance between Hepatitis B patients and healthy control subjects.

Because ICG-elimination depends strongly on hepatic blood flow, cardiovascular disease can affect ICG pharmacokinetics as well. As shown by Stenson et al. [67], there is a good correlation between cardiac output and hepatic blood flow. As a result, reduced cardiac output results in reduced ICG-elimination.

Also non-liver disease can alter ICG parameters. Andersen et al. [1] showed that ICG-clearance is significantly reduced in patients with chronic pancreatitis.

Understanding the alterations in ICG elimination is challenging because various factors affecting ICG parameters can be altered depending on disease. This can for instance be changes in blood flow, changes in functional liver tissue, or changes in protein binding properties e.g. via changes in bilirubin as mentioned in Sec. 1.5.

1.6.1 Cirrhosis

One of the most prominent liver diseases is cirrhosis. Cirrhosis is the final stage of many liver diseases. The most common causes are alcoholism, chronic hepatitis C virus infection and non-alcoholic fatty liver disease (NAFLD). Causes of liver cirrhosis vary geographically. Alcoholism and Hepatitis C appear most commonly in western countries, whereas in most parts of Asia and Africa chronic hepatitis remains the main cause of liver cirrhosis [21].

The pathological characteristics of cirrhosis include degeneration of hepatocytes and necrosis as well as a reduction of liver perfusion through increased resistance to portal blood flow. As such, liver cirrhosis will in most cases lead to portal hypertension [71].

In addition, cirrhosis also results in the formation of intrahepatic shunts. Intrahepatic shunts are blood-vessels that form inside the cirrhotic liver and bypass a portion of the portal and arterial blood supply past the metabolically active hepatocytes [71]. From the shunted blood, no ICG can be taken up by the liver, resulting in a reduction of ICG elimination capacity.

The severity of cirrhosis can be described using the Child-Turcotte-Pugh-Score (CTP). Based on a set of parameters, it assigns a score from 5-15 to a cirrhotic patient, where the more severe a patient's symptoms are the higher the score is. These parameters are serum bilirubin and albumin concentrations, prothrombin time, the International Normalized Ratio (INR) and the existence of ascites (increased amount of fluid in the peritoneal cavity due to liver cirrhosis). According to a patient's score, they are then classified as CTP-A (5-6 points), CTP-B (7-9 points) or CTP-C (10-15 points). An alternative score is the model

for end-stage liver disease (MELD) which has been widely used to predict survival of cirrhotic patients and to rank the priority of patients to receive liver transplantation. It is based on the INR, serum bilirubin concentration and the serum creatinine concentration [56].

A good correlation between CTP-score and ICG-elimination has been reported in several instances, reporting a reduction of ICG-elimination as CTP-score increases [15, 49, 47, 57]. Differences in ICG-elimination between cirrhotic patients and control subjects has been widely assessed [8, 6, 17].

Understanding how cirrhosis alters ICG elimination is of high clinical relevance. A better understanding of how ICG parameters change with increasing CPT and MELD score would be an important asset for the evaluation of patients.

1.7 Liver surgery (hepatectomy)

For many liver diseases, liver surgery is the only effective treatment with hepatic resection being the most common choice. Hepatic resection describes the partial excision of liver tissue in order to remove tumors or diseased liver tissue. In cirrhotic patients the most frequent indication of liver resection is HCC as well as cholangiocellular adenocarcinoma (CCA) or liver metastases.

The liver has the unique ability to regenerate its parenchymal tissue. Therefore a great amount of liver tissue (up to 70% in subjects with a healthy liver [11]) can be removed without causing liver failure. In general, it is the key objective of liver surgery to leave the patient with enough functional capacity of the future remnant liver to support regeneration. However, in subjects with underlying liver disease, the risk of postoperative complications is much higher and preoperatively assessed liver function may not be reliable for predicting future liver functional capacity. As a result, deciding if a patient is eligible for hepatic resection poses a great challenge.

Although there is a consensus that patients with advanced liver cirrhosis (CTP-C) are not eligible for hepatic resection, there is no clear consensus how to manage patients with less severe liver disease [11, 23]. Dynamic liver function tests such as ICG pharmacokinetic parameters, scoring systems like the Child-Turcotte-Pugh-Score or MELD, existence of portal hypertension or ascites and predicted liver remnant volume are factors included in the decision making process.

In many instances, ICG kinetics have been shown to be reliable indicators when deciding the course of a patients treatment, including liver surgery. Hemming et al. [24] showed that in contrast to other parameters ICG-clearance successfully predicted postoperative mortality in cirrhotic patients undergoing hepatic resection. Nonami et al. [51] showed that ICG-clearance is a very good prognostic marker of post-hepatectomy liver failure. Haeghe et al. [22] were able to show that preoperative reduced ICG-PDR and increased ICG-R15 significantly predict post-operative liver dysfunction. Further, they showed that an ICG-PDR of $<10\%/\text{min}$ or ICG-R15 $>20\%$ on postoperative day 1, predicted poor postoperative outcome. Overall ICG pharmacokinetic parameters provide important clinical information in the context of hepatic resection.

As described in Sec. 1.4 ICG elimination depends strongly on hepatic blood flow. Because removing liver volume affects hepatic perfusion (total hepatic blood flow through a reduced volume often in combination with changes in

portal pressure and tissue resistance), and because removing functional liver parenchyma will itself reduce the liver's ability to remove ICG from the blood, liver resection has a strong effect on ICG pharmacokinetics.

Multiple studies measured ICG elimination in the context of hepatectomy. Thomas et al. [70] measured ICG-PDR intraoperatively under trial clamping of inflow to those liver sections that were to be removed. This was in order to simulate post-hepatectomy liver function. They found significant correlation between post-hepatectomy and intraoperative ICG-PDR, suggesting that intraoperative ICG measurements under trial clamping can predict postoperative liver function. As a result, this may enable the surgeon conducting the resection to alter their strategy during the operation. Ohwada et al. [52], Okochi et al. [53] and Sunagawa et al. [69] all found significant correlation between postoperatively measured ICG-kel and estimated remnant ICG-kel, calculated by multiplying the remnant liver volume with the preoperative ICG-kel. Wakabayashi et al. [74] found a good correlation between preoperatively measured ICG-R15 and post-hepatectomy remnant liver volume in cirrhotic patients.

Despite these successes the remnant functional capacity based on ICG pharmacokinetics is challenging to predict in hepatectomy due to the complex interplay of removed liver tissue, altered perfusion and preliminary tissue damage (e.g. cirrhosis).

1.8 Physiological-based pharmacokinetic model (PBPK)

The complex interplay between changes in liver perfusion, effects of plasma proteins (e.g. via bilirubin), changes in liver disease (e.g. cirrhosis) and liver surgery (e.g. hepatectomy) on ICG elimination is difficult to understand.

Computational modeling allows to simulate the behavior of such complex systems and evaluate changes systematically *in silico*. This allows to gain new insights and elucidate underlying mechanisms. In the context of this project we were interested in how the elimination of ICG is influenced by factors such as liver perfusion or liver disease (cirrhosis) and how this affects liver function in liver surgery.

To this end, a physiological-based pharmacokinetics model (PBPK) model of ICG elimination was developed (see Sec. 3.2). PBPK models are based on a set of parameters that represent real aspects of the physiology of a subject (i.e. body weight, blood flow, tissue volumes). Using clinical data, many of these model parameters can be readily personalized. PBPK models are based on ordinary differential equations that can be solved numerically. This allows to predict the time course of ICG concentrations in the various compartments of the model such as plasma or liver. PBPK models are uniquely suited to study the dependency of ICG pharmacokinetics on plasma proteins, blood flow and liver disease.

1.9 Question, scope and hypotheses

Within this project the effects of blood flow, plasma proteins (effect of bilirubin), disease (cirrhosis), physiological factors and hepatic surgery (hepatectomy) on ICG elimination were studied by the means of computational modeling. Specifically, a PBPK model of ICG was developed to study the following questions:

- (i) What is the effect of blood flow changes on ICG elimination?
- (ii) What are the effects of changes in bilirubin on ICG elimination?
- (iii) How is ICG elimination changed in cirrhosis?
- (iv) How are ICG pharmacokinetic parameters changed in hepatectomy?

Our main objective was to describe the various influences on ICG elimination with a single consistent computational model and apply the model to clinically relevant questions such as: How does survival in hepatectomy correlate with ICG parameters? How do ICG parameters change with CTP scores?

2 Methods

Within this work the ICG elimination was studied by the means of a physiological-based pharmacokinetics model. The model was parameterized and validated using ICG time courses and data curated from published clinical studies.

The following methods were applied: Calculation of pharmacokinetic parameters from ICG time courses (Sec. 2.1), curation of ICG data for model parameterization and validation (Sec. 2.2), development of a physiological-based pharmacokinetic model (Sec. 2.3), parameter fitting of model parameters (Sec. 2.4), uncertainty analysis (Sec. 2.5) and sensitivity analysis (Sec. 2.6).

2.1 ICG pharmacokinetics parameters

For the evaluation of liver function based on ICG time courses, a set of pharmacokinetic parameters is calculated from the concentration-time curve. The same parameters are calculated either from clinically measured time courses or simulated time courses. The ICG pharmacokinetic parameters are the following:

Maximum concentration (cmax) The maximum concentration c_{max} [$\mu\text{mole/l}$] is the highest value of ICG plasma concentration reached in the concentration-time curve.

Time of maximum concentration (tmax) The time of maximum concentration t_{max} [min] is the time point when the plasma concentration reaches the maximum concentration c_{max} .

Volume of distribution (V_d) The volume of distribution V_d [l] is the volume that would be necessary to hold the total amount of drug in the body at the concentration that is measured in plasma. Because ICG does not leave the systemic circulation except when taken up by the liver, the volume of distribution is a good approximation of plasma volume. It is calculated as

$$V_d = AUC_{\text{inf}} * kel \quad (8)$$

with AUC_{inf} being the area under the concentration time curve extrapolated to infinity and kel the elimination rate.

Elimination rate (kel) The elimination rate kel [1/min] is the amount of drug that is removed from the body per minute. It is calculated by fitting the concentration-decay-curve to an exponential function: $C_{ICG}(t) = C_0 \cdot e^{-kel \cdot t}$.

ICG-PDR ICG-PDR [%/min] is essentially the same as the elimination rate kel but reported in different units.

Clearance (Cl) The clearance Cl [ml/min] describes the amount of blood or plasma that is cleared from the given substance per minute. It is calculated as:

$$Cl = V_d \cdot kel \quad (9)$$

ICG-R15 ICG-R15 [%] is the fraction of ICG, that has not been eliminated after 15 minutes and can be calculated via:

$$\text{ICG - R15} = \frac{C(15)}{C_{max}} \cdot 100 \quad (10)$$

In some studies alternative time points for ICG-R are reported, e.g., ICG-R20 [%] corresponding to 20 minutes.

Half-life ($t_{1/2}$) The half-life [min] of ICG is the time it takes for ICG concentration to reach half of the concentration. The half-life $t_{1/2}$ is calculated from the elimination rate kel via:

$$t_{1/2} = \frac{\ln(2)}{kel} \quad (11)$$

Extraction-ratio (ER) The extraction-ratio ER [-] is the fraction of drug, that is removed from the plasma after a single pass through the liver. When the plasma ICG concentration is in a steady-state it can be calculated as follows:

$$ER = \frac{C_{ar} - C_{hv}}{C_{hv}} \quad (12)$$

C_{ar} is the concentration of ICG in arterial blood, C_{hv} the concentration in hepatic venous blood.

2.2 ICG data

After formulating the main questions of this study (see Sec. 1.9) an extensive literature search was performed to find experimental data related to them. The main focus were published studies that reported ICG-specific parameters such as ICG-PDR or ICG-R15 and/or ICG pharmacokinetic time courses. Additional information of relevance were cardiovascular parameters such as cardiac output or hepatic blood flow as well as data on plasma proteins (albumin) and bilirubin. The search was performed for healthy control groups, subjects with liver disease (with special focus on cirrhosis) and liver surgery (main focus on hepatectomy).

Based on the publications a large data base of ICG pharmacokinetics data in Humans was established which was used in this project for model calibration and validation.

2.2.1 Data curation

A major task in the project was the curation of relevant data from the literature and establishing a standardized representation of the clinical information and data.

This was achieved by encoding all data in a recently established pharmacokinetics database (PK-DB; <https://pk-db.com>) [20]. PK-DB was used to encode the information on (i) patient characteristics (e.g. age, health status, medication, bilirubin), (ii) applied interventions (e.g. ICG dosing, route of application); (iii) measured ICG time-courses; (iv) ICG pharmacokinetic parameters (e.g. elimination rate, clearance, half-life time).

The information that these clinical studies provided was curated through a standardized curation process. This included encoding subject and group

characteristics, applied interventions, measured pharmacokinetic time-courses and pharmacokinetic parameters. As part of the process all data points were manually digitized.

Using an existing data base and data model allowed simple integration of the curated data with the developed model, by reusing existing workflows for integration of the data with the model. For more information on PK-DB and the curation process we refer to Grzegorzewski et al. [20].

2.3 Physiological-based pharmacokinetics models (PBPK)

Within this work a PBPK model was developed. The model is a deterministic ordinary differential equation (ODE) model. The model was solved numerically using an ODE solver, resulting in time course predictions from a given initial condition and model parameterization.

The model was developed and encoded using the Systems Biology Markup Language (SBML) [26, 34]. SBML is an XML-based format for representing biological models using a process based description. The models are defined as a set of species (metabolites), compartments (organs and blood compartments) and reactions (processes such as metabolic reactions and blood transport). The software sbmlutils [39] was used to develop the model which was simulated using sbmlsim [38] based on the high-performance SBML simulator libroadrunner [65].

An existing template whole-body model was adapted to describe the distribution and systemic circulation of ICG. An organ model of the liver for ICG uptake and bile excretion was developed and coupled to the whole-body model using SBML hierarchical model composition [64]. For simulation the hierarchical model was flattened into a single SBML model. A detailed description of the developed model is provided in the results in Sec. 3.2.

2.4 Parameter fitting

A subset of model parameters was determined using parameter fitting via solving an optimization problem. Hereby, the objective is to adjust the model's parameters in a manner that minimizes the residuals r between model predictions (observables) and experimental data. This optimization problem was solved using SciPy's least_squares method (a local optimization method) and the differential evolution algorithm (a global optimization method) [73]. For the objective cost function F depending on the parameters \vec{p} a simple L2-Norm was used consisting of the sum of weighted residuals

$$F(\vec{p}) = 0.5 \cdot \sum_{i,k} (w_k \cdot w_{i,k} \cdot r_{i,k}(\vec{p}))^2 = \sum_{i,k} (w_k \cdot w_{i,k} \cdot (y_{i,k} - m_{i,k}(\vec{p})))^2 \quad (13)$$

where:

$r_{i,k} = (y_{i,k} - m_{i,k}(\vec{p}))$ = the residual of time point i in time course k for model prediction $m_{i,k}(\vec{p})$ and the corresponding data point $y_{i,k}$

$w_{i,k}$ = the weighting of the respective data point i in timecourse k based on the error of the data point.

w_k = the weighting factor of time course k .

The final parameter set was determined using 250 runs of the local least square optimization.

2.5 Uncertainty analysis

To evaluate the uncertainty of the model predictions an uncertainty analysis was performed for a subset of simulations. Each model parameter was changed individually by $\pm 25\%$. From the set of resulting time courses the mean, standard deviation (SD) and minimum and maximum values at each time point were calculated. These uncertainty areas were displayed as shaded areas. The effect of this uncertainty on ICG pharmacokinetic parameters was evaluated by calculating the mean and standard deviation of the pharmacokinetic parameters that result from each of the simulations.

Parameters corresponding to physical constants (such as molecular weights) and dosing were not varied in the uncertainty analysis, as well as parameters responsible for conservation conditions like the fractional blood flow through the lung (must be 1).

2.6 Sensitivity analysis

In a sensitivity analysis, the influence of each model parameter on the resulting model prediction was evaluated. By varying each parameter p_i by 10% in both directions the sensitivity $S(q_k, p_i)$ of any ICG pharmacokinetic parameter q_k was calculated for each parameter as:

$$S(q_k, p_i) = \frac{q_k(p_{i,0}) - q_k(p_{i,\Delta})}{p_{i,0} - p_{i,\Delta}} \quad (14)$$

where $p_{i,\Delta}$ is the changed model parameter.

The same parameters that were excluded form the uncertainty analysis (see Sec. 2.6) were excluded from the sensitivity analysis.

3 Results

Within this project ICG pharmacokinetics were studied by the means of a physiological-based pharmacokinetics model. The model was parameterized and validated using ICG time courses and data curated from published clinical studies.

First, the curated ICG data is presented (Sec. 3.1) followed by a detailed description of the developed model (Sec. 3.2) and the results of the parameter fitting (Sec. 3.3). An overview of the model performance with reference simulation results is given (Sec. 3.4). In Sec. 3.5 the model is applied to study (i) ICG elimination in disease (cirrhosis) (Sec. 3.5.1); (ii) blood flow dependency of ICG elimination (Sec. 3.5.2); (iii) dependency on plasma proteins (bilirubin); and (iv) ICG elimination in hepatectomy. Finally a sensitivity analysis of the model is presented (Sec. 3.6).

3.1 ICG data

A wide range of heterogeneous data was curated for model building (parameterization) and subsequent model validation (comparison of model predictions against clinical data). An overview of the 36 studies curated in this project is provided in (Tab. 2). All data is freely available from <https://pk-db.com>.

Table 2: Overview of studies used for the parameterization and validation of the model. Data from **bold** studies was used in the parameter fitting of the model (see Sec. 3.3). All data is available at <https://pk-db.com>.

Study	Fit	ICG-protocol	Used in	Description
Andersen1999 PKDB00386 PMID: 10499483	✓	Bolus: 0.5 mg/kg	3.4.2	Pharmacokinetic time course of ICG-disappearance in chronic pancreatitis and healthy subjects.
Branch1976 PKDB00387 PMID: 1277728	-	Bolus: 0.5 mg/kg	3.5.3	Clearance of ICG in healthy subjects and chronic liver disease (cirrhosis, hepatitis).
Burns1991 PKDB00388 PMID: 1848168	✓	Bolus: 0.5 mg/kg; Infusion: 0.25 mg/min	3.4.2, 3.5.1	ICG pharmacokinetics in healthy subjects and patients with liver disease.
Caesar1961 PKDB00389 PMID: 13689739	✓	Bolus: 0.5 mg/kg; Infusion: 0.5 mg/min	3.5.1, 3.5.3	Measuring hepatic blood flow and assessing hepatic function by ICG pharmacokinetics.
Cherrik1960 PKDB00390 PMID: 13809697	-	Bolus: 0.5 mg/kg	3.5.1	ICG pharmacokinetics in healthy subjects and patients with liver disease.
Chijiwa2000 PKDB00391 PMID: 10773154	✓	Bolus: 0.5 mg/kg	3.4.2	Biliary excretion of ICG and ATP-dependency of ICG pharmacokinetics.
DOnofrio2014 PKDB00392 PMID: 24834884	-	Bolus: 0.5 mg/kg	3.5.3	Comparison between perfusion CT and ICG-R15/ICG-PDR as an estimation of liver functional reserve for patients undergoing hepatectomy.
Figg1995 PKDB00393 PMID: 8602375	-	Bolus: 0.5 mg/kg	3.5.1	Comparison of methods to assess hepatic function including CTP-score and ICG-clearance

Study	Fit	ICG-protocol	Used in	Description
Gadano1997 PKDB00394 PMID: 9083919	✓	Infusion: 0.4 mg/min (controls); 0.8 mg/min (cirrhotics). Additional priming dose.	3.5.2, 3.5.1	ICG-clearance and extraction-ratio and their dependency on hepatic bloodflow in healthy subjects and in patients of hepatic fibrosis and cirrhosis.
Grainger1983 PKDB00395 PMID: 6822056	✓	Bolus: 0.25 mg/kg	3.4.2	Non-invasive measurement of hepatic blood flow using ICG extraction-ratio.
Grundmann1992 PKDB00396 PMID: 1482735	✓	Bolus: 0.3 mg/kg	3.4.2, 3.5.2	Effect of anesthetics on ICG-pharmacokinetics and hepatic blood flow.
Herold2001 PKDB00397 PMID: 11169069	-	Bolus: 0.5 mg/kg	3.5.1	Comparison of liver function tests. Correlation between CTP-score and ICG-kel in healthy subjects and cirrhotic patients.
Huet1980 PKDB00398 PMID: 7398188	-	Bolus: 0.5 mg/kg	3.5.2	Effect of smoking and hepatitis B on ICG pharmacokinetics with estimates of hepatic blood flow.
Huet1983 PKDB00399 PMID: 6629320	-	Bolus: 0.5 mg/kg	3.5.2	ICG-pharmacokinetics in cirrhosis and chronic hepatitis with measurements of hepatic blood flow.
Kamimori2000 PKDB00299 PMID: 10883415	✓	Bolus: 0.5 mg/kg	3.4.2	Effect of the menstrual cycle on ICG pharmacokinetics.
Kanstrup1987 PKDB00400 PMID: 3816112	-	Infusion: 0.2 mg/min	3.5.2	Blood flow dependency of ICG-clearance.
Kawasaki1988 PKDB00401 PMID: 3396264	-	Bolus: 0.5 mg/kg	3.5.3	ICG-clearance in healthy subjects and patients of liver fibrosis and cirrhosis.
Keiding1993 PKDB00402 PMID: 8151094	-	Infusion: 0.08 mg/min	3.5.1	Effect of changing plasma protein concentrations on ICG-extraction.
Klockowski1990 PKDB00403 PMID: 2146057	✓	Bolus: 0.5 mg/kg	3.4.2	Effect of isradipine and diltiazem on ICG-pharmacokinetics.
Leevy1962 PKDB00404 PMID: 14463639	✓	Infusions: 0.3 and 1.5 mg/min/m ² with priming dose.	3.4.2, 3.5.2, 3.5.3	Estimation of hepatic blood flow using ICG.
Leevy1967 PKDB00405 PMID: 6071462	-	Bolus: 0.5 mg/kg and 5.0 mg/kg	3.5.1	Estimation of liver function with ICG. Dose dependency of ICG-PDR.
Martin1975 PKDB00406 PMID: 1208580	-	Bolus: 0.5, 2.0, 3.5 and 5.0 mg/kg	3.4.3	Differences in ICG-pharmacokinetics in men and women at varying ICG-doses.
Martin1976 PKDB00407 PMID: 814028	-	Bolus: 0.5, 2.0, 3.5 and 5.0 mg/kg	3.4.3	ICG-pharmacokinetics in patients with Gilbert's Syndrome.
Meijer1988 PKDB00408 PMID: 3181282	✓	Bolus: 0.5, 1.0 and 2.0 mg/kg	3.4.2, 3.4.3	Biliary excretion of ICG at different doses.
Moeller1998 PKDB00409 PMID: 9691928	-	Infusion: Rate not reported	3.5.1	Arterial hypoxaemia in cirrhosis. Correlation between ICG-clearance and CTP-score.

Study	Fit	ICG-protocol	Used in	Description
Moeller2019 PKDB00410 PMID: 30221390	-	Infusion: 0.2 mg/min with priming dose	3.5.1	Correlation between ICG-pharmacokinetics and CTP-score.
Niemann2000 PKDB00414 PMID: 10801242	✓	Bolus: 10 mg	3.4.2	ICG- pharmacokinetic time course under administration of propranolol.
Ohwada2006 PKDB00412 PMID: 16498606	-	Bolus: 20 mg	3.5.4	Prediction of postoperative liver functional capacity based on ICG-pharamcokinetics.
Okochi2002 PKDB00415 PMID: 11855925	-	Bolus: 20 mg	3.5.4	Comparison of preoperative and postoperative ICG-pharmacokinetics. Prediction of postoperative liver functional capacity based on ICG-pharamcokinetics.
Sakka2006 PKDB00413 PMID: 16544120	-	Bolus: 0.5 mg/kg	3.6	Relation between ICG-PDR and ICG-clearance in patients with non-liver disease.
Seyama2009 PKDB00416 PMID: 19208031	-	Bolus: Not reported	3.6	Assessment of liver function for safe hepatic resection. Prediction of survival after hepatectomy based on ICG-R15.
Soons1991 PKDB00411 PMID: 1768562	✓	Infusion: 2.0, 0.5, 1.0 mg/min (consecutive)	3.4.2	Assessment of hepatic blood flow in healthy subjects by continuous infusion of ICG.
Stockmann2009 PKDB00417 PMID: 19561474	-	Bolus: 0.5 mg/kg	3.5.4	Prediction of postoperative liver functional capacity based on ICG-pharamcokinetics.
Sunagawa2021 PKDB00418 PMID: 33052632	-	Bolus: 20 mg	3.5.4	Prediction of postoperative liver failure based on ICG-kel measurements.
Thomas2015 PKDB00419 PMID: 25581073	-	Bolus: 0.25 mg/kg	3.5.4	Intraoperative prediction of postoperative liver functional capacity using trial-clamping and ICG-pharmacokinetics.
Wakabayashi2004 PKDB00420 PMID: 15013363	-	Bolus: 0.5 mg/kg	3.5.4	Correlation between preoperative ICG-R15 and estimated liver remnant. Prediction of survival based on ICG-R15.

3.2 Computational model of ICG

3.2.1 Physiological based pharmacokinetics model (PBPK)

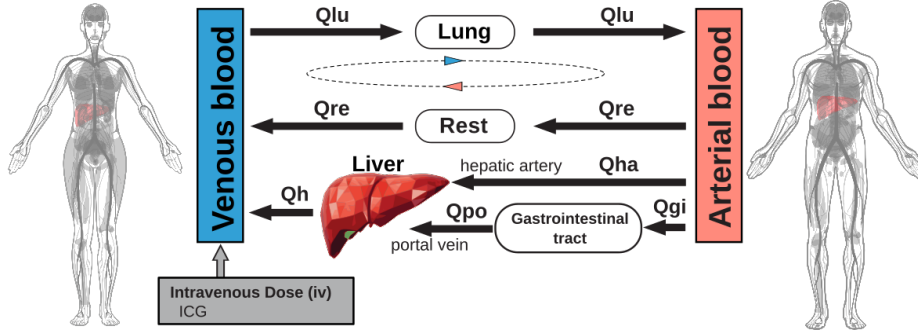


Figure 3: Overview of the whole-body model showing the blood circulation through the compartments.

To simulate the distribution and elimination of ICG in the human body two models were developed: (i) A whole-body model (Fig. 3) consisting of multiple tissues and plasma compartments which are connected via blood flow. The whole-body model describes the distribution of substances in the body and to the organs. (ii) A liver model (Fig. 4) which describes hepatic uptake of ICG, biliary excretion of ICG and transport of ICG into the feces. The two models were coupled to describe whole-body distribution and hepatic elimination of ICG.

An overview of important model parameters is provided in Tab. 4. The liver model, whole-body model and coupled liver-whole-body models are available as SBML from <https://github.com/adriankl/icgmodel> alongside the final results of the parameter fit.

3.2.2 Distribution

The whole-body model (Fig. 3) consists of the minimal number of tissues relevant for the description of ICG kinetics. Because no other tissue besides the liver can take up ICG the remaining tissues such as heart, muscle, adipose tissue or kidneys were pooled in a single rest compartment.

The two main plasma compartments in the whole-body model are the venous blood and arterial blood. After an intravenous dose to the venous compartment ICG is distributed to all blood compartments. ICG transport through the cardiovascular system is implemented in the model as an irreversible transport reaction based on a blood flow parameter Q_i and the ICG concentration C_i of the respective compartment i from which the blood is transported to the next compartment:

$$v_i = Q_i \cdot C_i \quad (15)$$

First, venous blood is transported through the lung into the arterial blood compartment. After entering the arterial blood compartment, ICG is then distributed to the liver, the gastrointestinal tract and a rest compartment. From

the gastrointestinal tract blood empties into the portal vein that leads into the liver. This venous blood supply is added to the arterial supply of the liver. The hepatic vein transports blood out of the liver back into the venous blood compartment. It is important to note that in the model the liver is split into a tissue compartment that represents the liver parenchyma and a blood compartment that represents the blood vessels in the liver.

3.2.3 Blood flow

Total blood flow in the model is defined by the cardiac output Q_{CO} as

$$Q_{CO} = BW \cdot COBW \quad (16)$$

where BW is the body weight and $COBW$ is the cardiac output normalized to the body weight. The blood flow through each organ is then calculated as

$$Q_{organ} = Q_{CO} \cdot fQ_{organ} \quad (17)$$

where fQ_{organ} is the fractional tissue blood flow for the specific organ. The values for each organ are provided in Table 3.

Table 3: Fractional tissue blood flows. By multiplying these with the cardiac output Q_C , tissue blood flow through each organ is defined.

Organ	Parameter	Value [-]
Liver	fQ_h	0.255
Gastrointestinal tract	fQ_{gi}	0.19
Rest	fQ_{re}	0.555
Lung	fQ_{lu}	1

Multiple conservation conditions hold in the model to ensure mass and flow balance. First the sum of blood flows from the arterial to the venous compartment must equal the sum of flows in the reverse direction:

$$Q_{CO} = Q_{lu} = Q_h + Q_{re} \quad (18)$$

As a consequence of this condition and due to the cardiac output being constant changes in hepatic blood flow are compensated by inverted changes of the blood flow through the rest of the body.

All flow into an organ must be equal to flow out of the organ. I.e. the portal blood flow is equal to the gastrointestinal tract blood flow:

$$Q_{po} = Q_{gi} \quad (19)$$

The total blood flow through the liver is the sum of the blood flow through the hepatic artery and portal vein:

$$Q_h = Q_{ha} + Q_{po} \quad (20)$$

resulting in the hepatic arterial blood flow as:

$$Q_{ha} = Q_h - Q_{po} \quad (21)$$

To simulate the dependency of ICG elimination on hepatic blood flow two different approaches were taken. (i) Hepatic blood flow Q_h and gastrointestinal tract blood flow were changed by a factor $f_{bloodflow}$.

$$Q_h = Q_{CO} \cdot fQ_h \cdot f_{bloodflow}$$

$$Q_{gi} = Q_{CO} \cdot fQ_{gi} \cdot f_{bloodflow}$$

Through this, portal and hepatic arterial blood flow are changed according to (19) and (21). The changes are compensated for by the blood flow through the rest of the body Q_{re} .

(ii) Systemic blood flow Q_{CO} was varied by a factor $f_{cardiac_output}$ thereby changing total blood flow and effectively changing hepatic blood flow.

$$Q_{CO} = BW \cdot COBW \cdot f_{cardiac_output}$$

As a result Q_{re} , Q_{lu} and Q_h are changed by the same factor as Q_{CO} .

3.2.4 Hepatic metabolism and biliary excretion

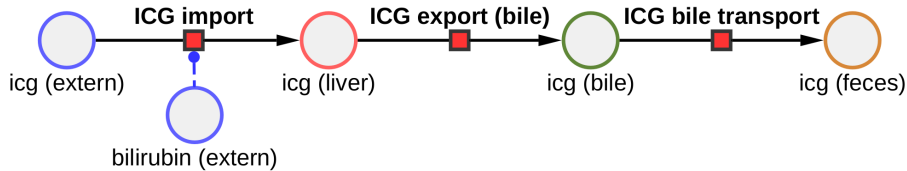


Figure 4: ICG liver model. ICG in the liver plasma compartment (icg (extern)) can be taken up into the liver tissue. Subsequently hepatic ICG is excreted in the bile from where it is excreted in the feces. The effect of bilirubin on ICG import was modeled as a competitive inhibition on the ICG import.

Hepatic uptake of ICG, biliary excretion and transport into the feces is described by the liver model (Fig. 4). As ICG enters the liver blood compartment, it can be taken up into the liver tissue compartment. The transport was modeled via an irreversible Michaelis-Menten equation:

$$v_{uptake} = V_{li} \cdot \frac{V_{max} \cdot [ICG_{ext}]}{K_m + [ICG_{ext}]} \quad (22)$$

The uptake rate scales with the volume of the liver V_{li} .

Biliary excretion is modeled as a second irreversible transport reaction from liver into the bile. The reaction velocity is also defined via an irreversible Michaelis-Menten equation:

$$v_{bile} = V_{li} \cdot \frac{V_{max} \cdot [ICG_{li}]}{K_m + [ICG_{li}]} \quad (23)$$

The transport into the feces is modeled by a first order kinetic.

$$v_{feces} = V_{li} \cdot V_{max} \cdot [ICG_{bi}] \quad (24)$$

Because there is no interaction with the intestinal tissue before ICG enters the feces, the intestinal tissue was not considered in the model. Because

ICG does not undergo enterohepatic circulation, no re-uptake of ICG from the intestinal contents is included in the model.

3.2.5 Plasma proteins (bilirubin)

So far no consensus exists which plasma proteins are responsible for the binding of ICG and how these plasma proteins affect ICG uptake (see Sec. 1.5). Implementing multiple binding proteins (albumin and lipoproteins consisting of many fractions) with varying affinities and concentration dependencies towards ICG posed a major challenge, especially because only very sparse data was available.

Consequently, we decided to remove the plasma proteins from the picture entirely and focus on the competitive inhibition of ICG hepatic uptake by bilirubin most likely mediated via plasma proteins. This competitive inhibition was implemented in the model by extending the hepatic uptake kinetic with a competitive inhibition term:

$$v = V_{li} \cdot \frac{v_{max} \cdot [ICG_{ext}]}{k_m \cdot (1 + \frac{[Bil]}{k_i}) + [ICG_{ext}]} \quad (25)$$

where:

$[Bil]$ = the plasma concentration of bilirubin

k_i = the inhibition constant of bilirubin for hepatic ICG-uptake

The dependency of ICG pharmacokinetics on bilirubin was simulated by varying the bilirubin concentration in the physiological range between 0.001 mmole/l and 0.3 mmole/l on a logarithmic scale.

Because changes in bilirubin plasma concentration happen very slowly (hours-days) compared to the time scale of ICG elimination (minutes), bilirubin was assumed in steady state and not modeled explicitly.

Table 4: Overview of important model parameters

Parameter	Description	Value	Unit
BW	Body weight	75	kg
$COBW$	Cardiac output per body weight	0.83	ml/s/kg
QC	Cardiac output resulting from $BW \cdot COBW$	3.75	l/min
HCT	Hematocrit	0.51	-
$Fblood$	Fraction of organ volume that is blood vessels	0.02	-
$FVgi$	Fractional tissue volume of the gastrointestinal tract	0.0171	l/kg
$FVli$	Fractional tissue volume of the liver	0.0210	l/kg
$FVlu$	Fractional tissue volume of the lung	0.0076	l/kg
$FVve$	Fractional tissue volume of the venous blood	0.0587	l/kg
$FVar$	Fractional tissue volume of the arterial blood	0.0184	l/kg
$[LI_bil_ext]$	Bilirubin concentration in the liver plasma	0.01	mM
$ICGIM_ki_bil$	Inhibition constant of bilirubin	0.02	mM

3.2.6 Liver disease (cirrhosis)

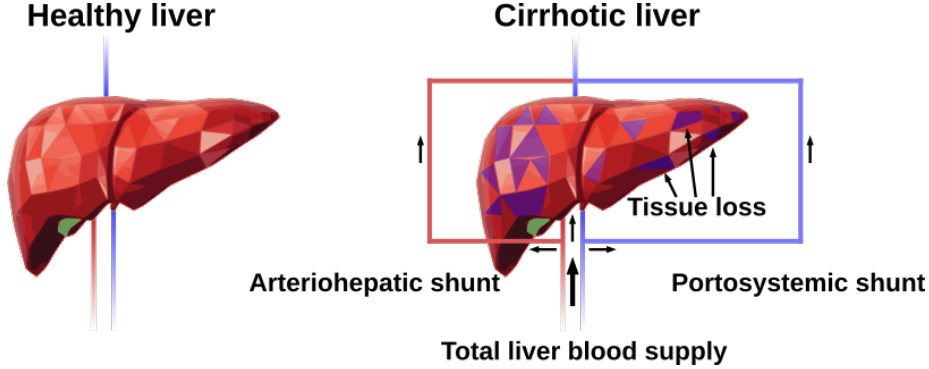


Figure 5: Overview of how liver cirrhosis was implemented in the model.

The model was adapted to allow the simulation of liver cirrhosis as an example liver disease.

The reference model, representing a healthy human subject, was adjusted to simulate cirrhosis by including a combination of functional tissue loss (due to scarring and necrosis in cirrhosis) and the formation of intrahepatic shunts, both key hallmarks of cirrhosis (see Sec. 1.6.1).

The loss of functional liver tissue was controlled via the parameter $f_{tissue_loss} \in [0, 1]$ which defines the fraction of parenchymal cell volume lost in the liver due to the disease. This parameter was implemented in a way that it does not reduce the liver blood volume, but exclusively the tissue.

For modeling arteriohepatic and portosystemic shunts two additional blood vessels were introduced into the model. They connect the hepatic artery and the portal vein directly to the hepatic vein. As a result, a part of the portal venous and arterial blood bypasses the active liver tissue and is emptied into the hepatic venous blood compartment, so that ICG can not be extracted (corresponding to *in silico* shunts). The amount of blood that flows through the shunts is controlled by the parameter $f_{shunts} \in [0, 1]$, which defines the fraction of blood bypassing the liver. The remaining blood ($1 - f_{shunts}$) reaches the liver tissue and ICG can be extracted.

To simulate various degrees of cirrhosis the parameters f_{shunts} and f_{tissue_loss} were varied in lockstep by coupling them into one parameter $f_{cirrhosis}$.

The following cirrhosis degrees were used in the simulations: healthy: $f_{cirrhosis}=0$; mild cirrhosis: $f_{cirrhosis}=0.2$; moderate cirrhosis: $f_{cirrhosis}=0.5$; severe cirrhosis: $f_{cirrhosis}=0.8$.

3.2.7 Liver surgery (hepatectomy)

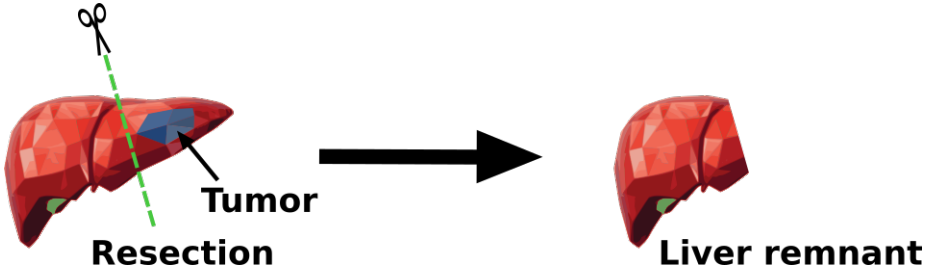


Figure 6: Overview of how hepatectomy was implemented in the model.

ICG pharmacokinetic parameters are an important clinical tool in liver surgery and are routinely applied to predict the functional capacity in hepatectomy (see Sec. 1.7). The developed model was applied to predict changes in ICG pharmacokinetic parameters under various degrees of liver resection.

Hepatectomy was simulated by performing an *in silico* removal of liver volume (tissue with corresponding vessels). More specifically, the model parameter $FVli$, corresponding to the fractional liver volume of the whole body, was varied between 10% (90% resection) and 100% (no resection) of its reference value of $0.021[l/kg]$.

The remaining parenchymal liver volume results as

$$V_{li_tissue} = BW \cdot FVli \cdot (1 - f_{tissue_loss}) \cdot (1 - Fblood) \quad (26)$$

with remaining liver volume as

$$V_{li} = BW \cdot FVli \cdot (1 - f_{tissue_loss}) \quad (27)$$

The parameter $Fblood$ describes the fraction of the organ consisting of vessels (2% of organ volume).

Because many subjects undergoing resection suffer from underlying liver disease the hepatectomies were simulated under varying degrees of cirrhosis as described above (see Sec. 3.2.6).

3.3 Parameter fitting

Parameter fitting of the model was performed using a subset of clinical data consisting of ICG time courses and extraction-ratio measurements. No ICG pharmacokinetic parameters were used in the model fitting process. An overview of the subset of data that was used in parameter fitting is provided in Tab. 5.

Table 5: Overview of the data used in parameter fitting. More information on these studies is provided in Tab. 2

Study	Used
Andersen 1999 [1]	ICG time course (plasma)
Burns 1991 [6]	ICG time course (plasma)
Caesar 1961 [8]	ICG extraction-ratio
Chijiwa 2000 [10]	ICG time course (bile excretion)
Grainger 1983 [18]	ICG extraction-ratio
Grundmann 1992 [19]	ICG time course (plasma)
Kamimori 2000 [29]	ICG time course (plasma)
Klockowski 1990 [37]	ICG time course (plasma)
Leevy 1962 [40]	ICG extraction-ratio; ICG time course (hv and ar)
Meijer 1988 [46]	ICG time course (plasma & bile excretion)
Niemann 2000 [50]	ICG time course (plasma)
Soons 1991 [66]	ICG time course (plasma)

The parameters that were fitted are depicted in Tab. 6 along with their respective values. Within this work only parameters for the transport kinetics of ICG in the liver and excretion in the bile were fitted. Physiological parameters of the existing whole-body template such as reference organ volumes and blood flows were not modified in the parameter fitting process.

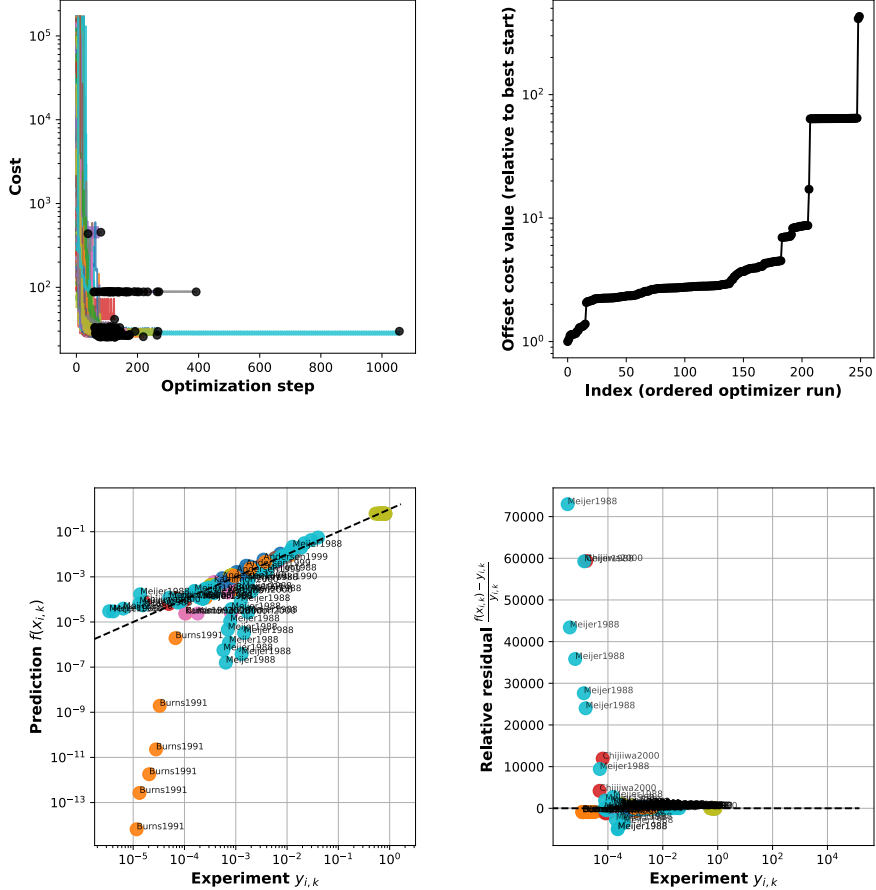


Figure 7: Parameter fitting results consisting of optimization traces, Waterfall plot, overview of predicted vs. experimental data and the corresponding residuals. For the final parameter set given in Tab. 6 250 least square optimizations were run.

An overview of the parameter fitting performance and results are provided in Fig. 7. A good improvement of the cost can be seen. Some local optima seem to exist. It is shown that all optimization-runs improve the cost. The overview of residuals from all simulations, that were used for the parameter fit, show that three simulations (Meijer1988, Chijiwa2000 and Burns1991) deviate significantly from the corresponding clinical data. The model is not yet able to accurately predict the biliary excretion of ICG at different doses (see Fig. 11 and 10). Further it is not able to describe long ICG plasma disappearance curves correctly. This is due to a second, slower phase of ICG elimination that occurs when the ICG plasma-concentration is low. However, as this effect has little influence on the application of ICG as a liver function test, this second phase is rarely measured. As a result, no efforts were made to implement this second phase of ICG elimination in the model.

Table 6: Fitted parameters used for modelling ICG hepatic uptake, biliary excretion and bile flow.

Parameter	Description	Value	Unit
LI_ICGIM_Vmax	V_{max} of liver import	2.25E-2	mmole/min/l
LI_ICGIM_Km	K_m of liver import	1.39E-2	mM
LI_ICGLI2CA_Vmax	V_{max} of bile excretion	9.58E-4	mmole/min/l
LI_ICGLI2CA_km	K_m of bile excretion	1.18E-2	mM
LI_ICGLI2BI_Vmax	V_{max} of bile transport	1.14E-4	1/min

Overall, 5 model parameters were fitted. Two of them determine the import of ICG in the liver, three determine the subsequent excretion in the bile. The agreement between fit data and model predictions improved substantially during parameter fitting and all data with the above-mentioned exceptions could be described very well after parameter fitting.

3.4 Model performance

To assess the model's behavior, first a reference simulation was performed for a bolus injection as well as a continuous infusion of ICG (see Sec. 3.4.1). Next, the model prediction of the training data was evaluated by comparing measured ICG time courses and extraction-ratios to the model predictions (see Sec. 3.4.2). In addition, the dose-dependency of ICG pharmacokinetic parameters was analyzed (see Sec. 3.4.3).

3.4.1 Reference simulation

With the fitted model, we are able to predict ICG pharmacokinetics in its reference state. To simulate a plasma disappearance curve a bolus dose of 0.5 mg/kg ICG was administered. To simulate a constant ICG infusion, an infusion rate of 2 mg/min ICG was injected. The resulting time courses are shown in Fig. 8.

After a bolus administration of 0.5 mg/kg ICG, the ICG venous plasma concentration quickly reaches its peak value and returns to baseline after 30 minutes. The liver extracts ICG resulting in a drop in ICG concentration between arterial plasma and hepatic vein. From the arterial and hepatic venous plasma concentrations the ICG extraction-ratio of ca. 0.6 can be calculated. The ICG extraction-ratio reaches steady state quickly. In the time course of ICG in the liver tissue we can see a complete change of timescale in comparison to the plasma concentrations. ICG in the liver returns to baseline only after around 3 hours. This is due to the biliary excretion being much slower than the hepatic uptake, as can be seen in the bottom panel of Fig. 8.

A similar analysis was performed for a constant infusion of 2 mg/min ICG. ICG venous plasma concentration reaches steady state after 25 minutes with a constant extraction-ratio of around 0.6. Similar to the bolus administration, it takes a much longer time for ICG in the liver tissue to reach steady state. Surprisingly, the biliary excretion rate has not completely reached steady state even after over 24 hours.

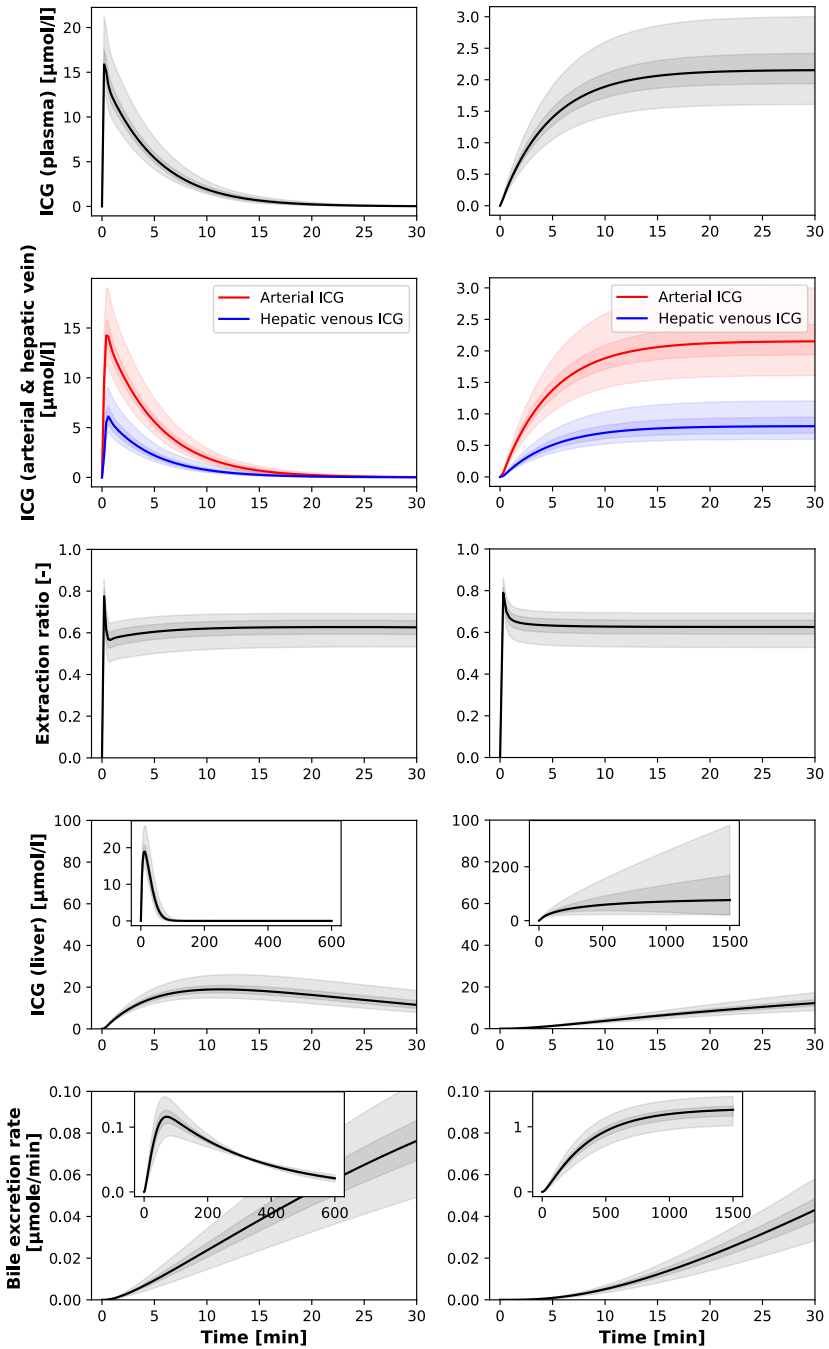


Figure 8: Reference simulation. Performance of the model in its reference state with the fitted parameters. Insets show differences in timescale. **Left:** an ICG bolus of 0.5 mg/kg **right:** a constant ICG infusion of 2 mg/min. Shaded areas show results of the uncertainty analysis.

From the simulated plasma disappearance curves ICG pharmacokinetic parameters can be calculated as described in Sec. 2.1. The results are shown in Tab. 7. In addition to the values calculated from the reference simulation, Tab. 7 shows the mean values and standard deviations resulting from the uncertainty shown in Fig. 8. Interestingly, ICG-R15 shows larger changes in the model parameters when comparing the value to the uncertainty mean than other pharmacokinetic parameters (Coefficient of variation of 28.6% compared to 9-10% for other parameters). A more in-depth analysis of the sensitivity of ICG-pharmacokinetics on the models parameters are provided in Sec. 3.6.

Table 7: ICG pharmacokinetic parameters calculated from the reference model simulation in Fig. 8. **Value:** Value resulting from the reference time course; **Uncertainty:** Mean and standard deviation and coefficient of variation (Mean \pm SD (CV)) calculated from the uncertainty in the reference time course (shaded area).

Parameter	Value	Uncertainty	Unit
ICG-PDR	21.30	21.31 \pm 2.08 (9.8%)	%/min
ICG-R15	4.01	4.26 \pm 1.22 (28.6%)	%
ICG-t _{1/2}	3.25	3.28 \pm 0.32 (9.8%)	min
ICG-clearance	577.4	575.0 \pm 54.0 (9.4%)	ml/min

3.4.2 ICG timecourses

In a next step model predictions were compared to measured ICG time courses (Fig. 9). For the simulations body weights and dosing or injection protocols were adjusted as reported in the respective studies (no other model parameters were changed).

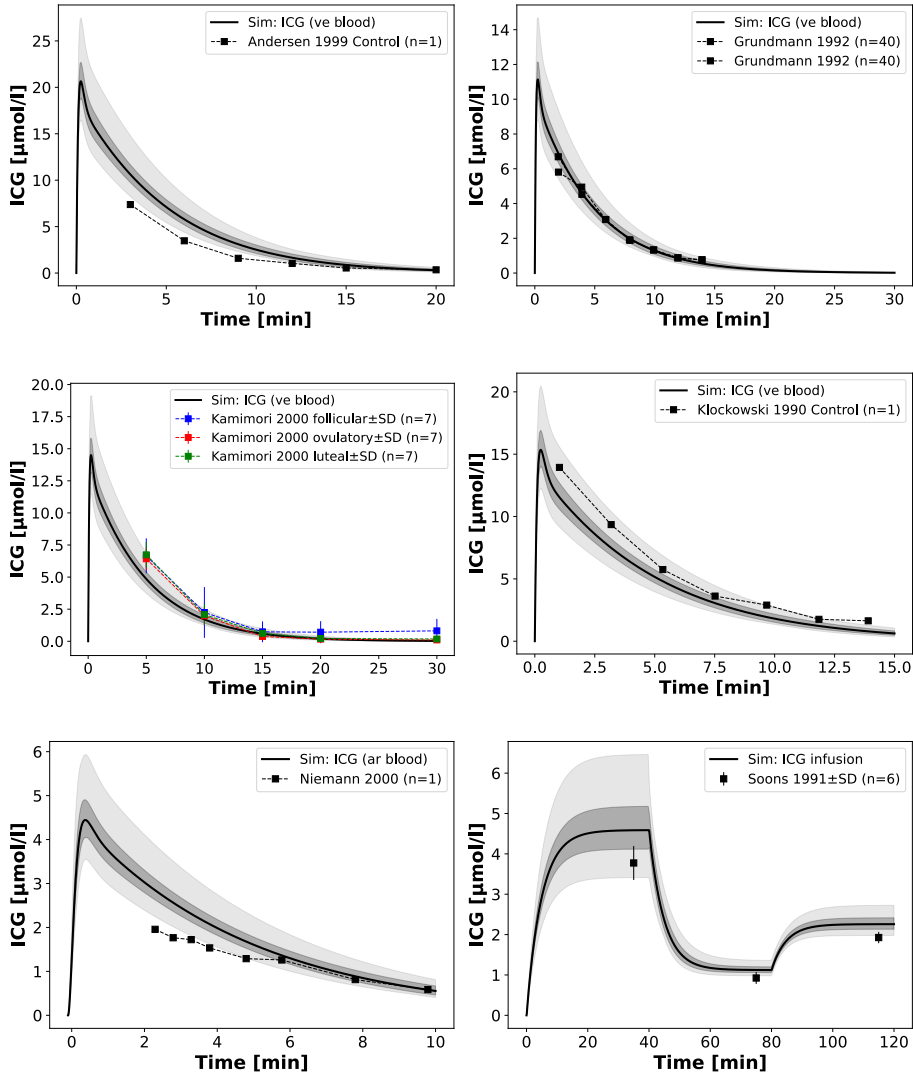


Figure 9: Simulation of ICG time courses. The model simulation was performed according to the dosing/infusion protocols used in the clinical studies [1, 19, 29, 37, 50, 66].

The model predictions for ICG plasma disappearance curves after an ICG bolus agree well with the clinical data [1, 19, 29, 37, 50]. In addition, more complex infusion protocols as reported in Soons et al. [66] are described well. The simulation describes the ICG plasma concentration time course under an

infusion protocol of three different infusion rates ($2.0 \rightarrow 0.5 \rightarrow 1.0$ mg/min, each for 40 minutes). Due to the high extraction-ratio of ICG, the plasma concentration is able to reach steady state quickly after each change in the infusion rate.

Next we were interested how the model performs in regard to biliary excretion of ICG. A simulation of the biliary excretion rate of ICG after a bolus administration was performed and the results were compared to data from Chijiwa et al. [10] (see Fig 10).

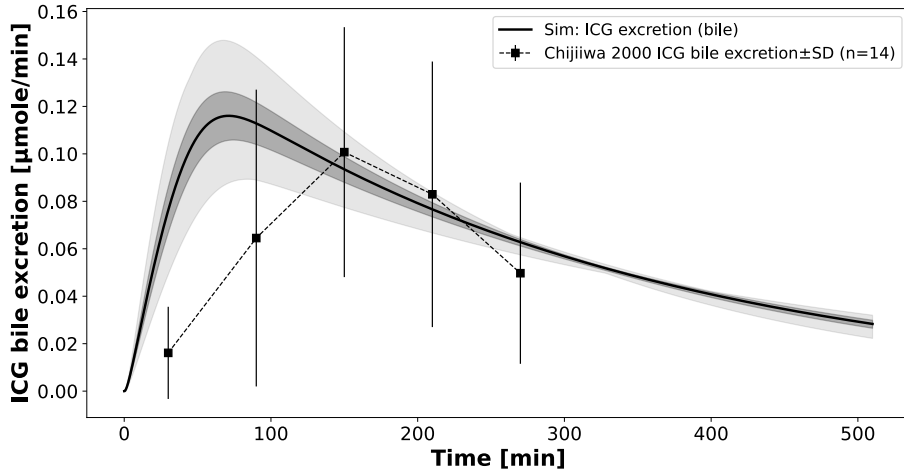


Figure 10: Time course simulation of the biliary excretion of ICG. The model prediction was compared to clinical data from Chijiwa et al. [10].

The model prediction agrees well with the clinical data and shows a clear difference in timescale to the plasma concentration time courses.

Furthermore, the ICG plasma concentration time course and the biliary excretion time course for three different doses of ICG was simulated in Fig. 11.

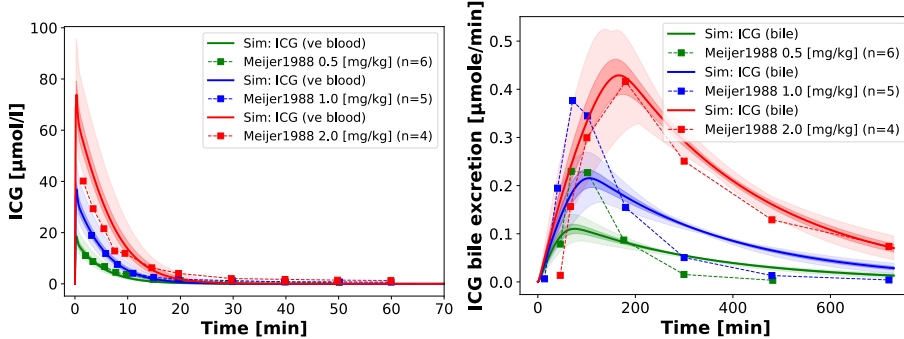


Figure 11: Time course simulation of the plasma disappearance curve and biliary excretion rate of ICG at three different doses (green - 0.5 mg/kg; blue - 1.0 mg/kg; red - 2.0 mg/kg). Clinical data from Meijer et al. [46].

The model prediction of the plasma concentration time courses compare well to the data from Meijer et al. [46] and the dose dependency is well described. The clinical data of the biliary excretion of ICG shows a nonlinear dependency on the administered dose, that the model can not reproduce. Instead, the model predicts a linear dose dependency and agrees with the reported data only for the high administration amount of 2.0 mg/kg ICG. This is caused by the simplified way of implementing biliary excretion in the model. With more clinical data and a more accurate model-representation of the biliary excretion rate of ICG, more accurate predictions would be possible.

Extraction-ratio ICG extraction-ratio is an important parameter when studying ICG pharmacokinetics. It describes the fraction of ICG that is removed in one passing through the liver. It is calculated based on the difference in ICG concentration between the hepatic vein and arterial blood as described in Sec. 2.1. The model prediction of the ICG extraction-ratio compared to clinical data is shown in Fig. 12.

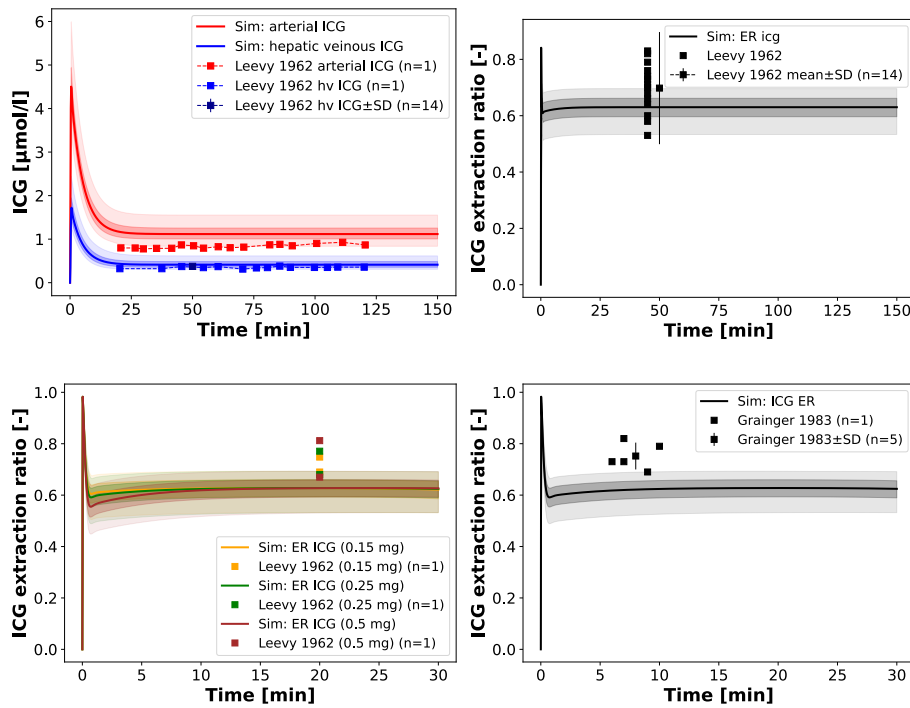


Figure 12: Simulation of hepatic venous and arterial ICG concentrations and extraction-ratios compared to clinical data from [40, 18].

The model accurately predicts the ICG extraction-ratio as well as the difference between the hepatic venous and arterial ICG concentrations. Fig. 12 (bottom left) shows that the ICG extraction-ratio does not depend on the administered dose at all, which the model is able to predict.

Overall, the model shows the ability to accurately predict ICG timecourses for venous and arterial plasma concentrations, for hepatic vein concentrations,

and extraction ratios when compared to clinical data. Especially plasma time-courses of icg after ICG bolus and ICG infusion are very well predicted by the model. This is a first important step in validating the model, because all ICG pharmacokinetic parameters are calculated from these plasma disappearance curves.

3.4.3 Dose dependency

The dependency of the pharmacokinetic parameters on the dose of ICG was studied. Although the pharmacokinetic timecourse of ICG changes with the administered dose, we did not find a significant dependency of ICG pharmacokinetic parameters on the dose in the clinically relevant range of ICG administration. A comparison of the model prediction to clinical data as well as a systematic analysis of the dose-dependency is provided in the supplement.

3.5 Model application

3.5.1 Disease (cirrhosis)

In order to simulate changes of ICG pharmacokinetics in cirrhosis, hepatic tissue loss and shunts were included in the model as described in Sec. 3.2.6.

First a systematic analysis of the effect of intrahepatic shunts (f_{shunts}), functional tissue loss (f_{tissue_loss}) and the combination of both ($f_{cirrhosis}$) on ICG pharmacokinetic parameters was performed (Fig. 13). All three parameters were varied from 0 (no effect) to 0.9 (severe effect).

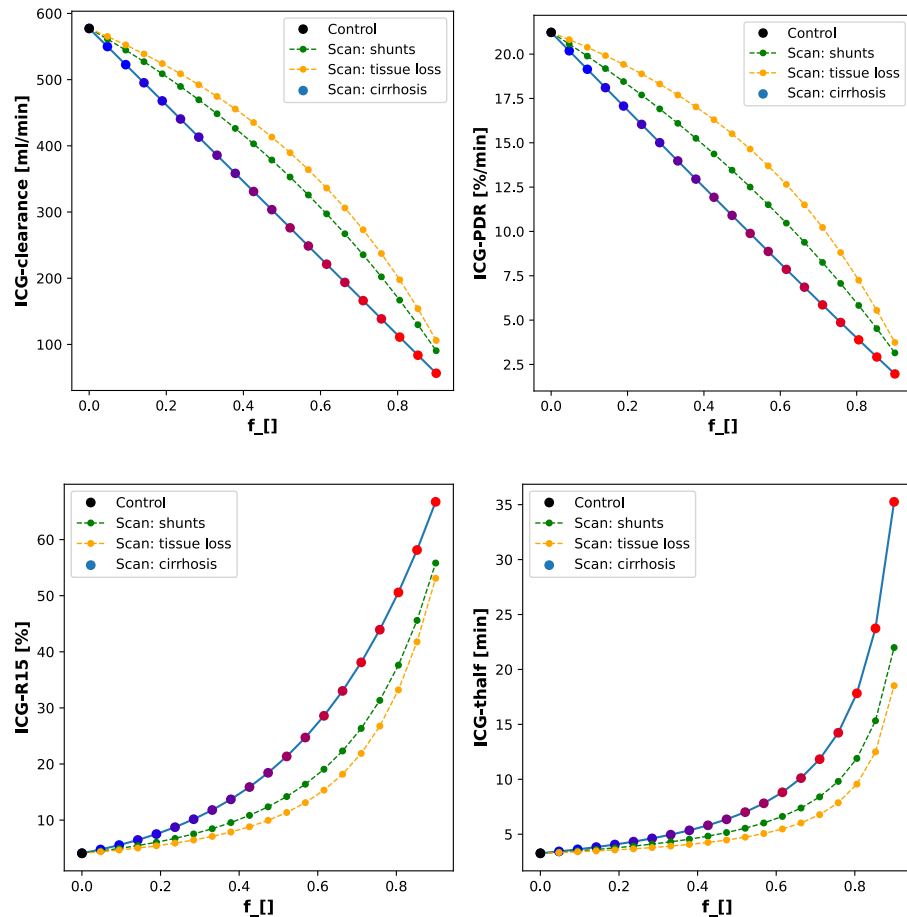


Figure 13: Systematic analysis of the individual effect of shunts (green) and tissue loss (orange) on ICG pharmacokinetic parameters as well as their combined effect (blue —→ red).

The results show a strong dependency of ICG pharmacokinetic parameters on these parameters. ICG-clearance and ICG-PDR both decrease with increasing degree of cirrhosis, while ICG-R15 and ICG-t_{1/2} increase. The loss of a fraction of functional liver tissue appears to have a smaller effect on ICG pharmacokinetic parameters than shunting of an equal fraction of blood past the

liver. When f_{shunts} and f_{tissue_loss} are both increased they combine to have a greater effect as when they are increased individually. This shows that the effects of shunting of blood and the loss of functional liver tissue are additive. For ICG-clearance and ICG-PDR the effects of both parameters combine to an almost linear dependency on $f_{cirrhosis}$. However, for ICG- $t_{1/2}$ and ICG-R15 the nonlinearity is not changed by the combination of shunts and tissue loss. In regard to ICG- $t_{1/2}$ and ICG-R15 shunts, tissue loss and cirrhosis up to around 0.4 (40%) have only a minor effect on the respective ICG parameters.

Having evaluated the effect of $f_{cirrhosis}$ on the model prediction of ICG parameters, a comparison of an ICG time course in a healthy subject and a cirrhotic subject was performed (Fig. 14).

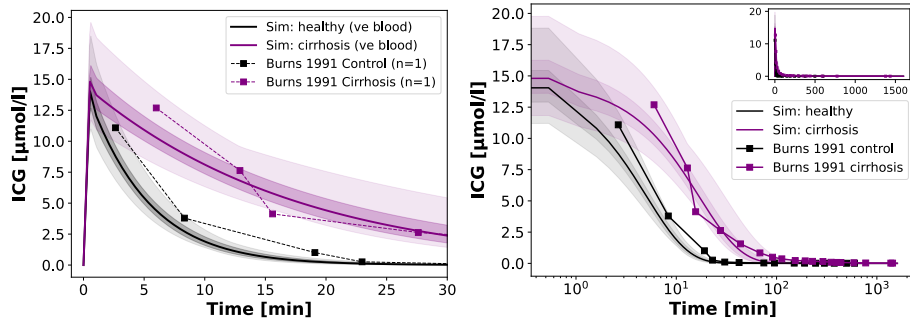


Figure 14: Simulation of ICG plasma disappearance curve compared to clinical data from Burns et al. [6]

By setting $f_{cirrhosis}$ to 0.7, the model prediction of an ICG time course in a cirrhotic patient agrees well with the clinical data from Burns et al. [6]. The main differences to the reference simulation are a marginally higher peak and a slower disappearance rate. As a result, ICG concentrations in the cirrhotic liver are higher than in the reference simulation, because ICG elimination is reduced.

The effect of cirrhosis on the ICG extraction-ratio has been studied in several instances [8, 16]. In Fig. 15 we analyzed the dependency of the ICG extraction-ratio on the degree of cirrhosis and compared the model prediction to clinical data. The simulation was performed for four different degrees of cirrhosis (healthy: $f_{cirrhosis} = 0.0$; mild cirrhosis: 0.2; moderate cirrhosis: 0.5; severe cirrhosis: 0.8). In Fig. 16 simulations were performed with individual $f_{cirrhosis}$ values.

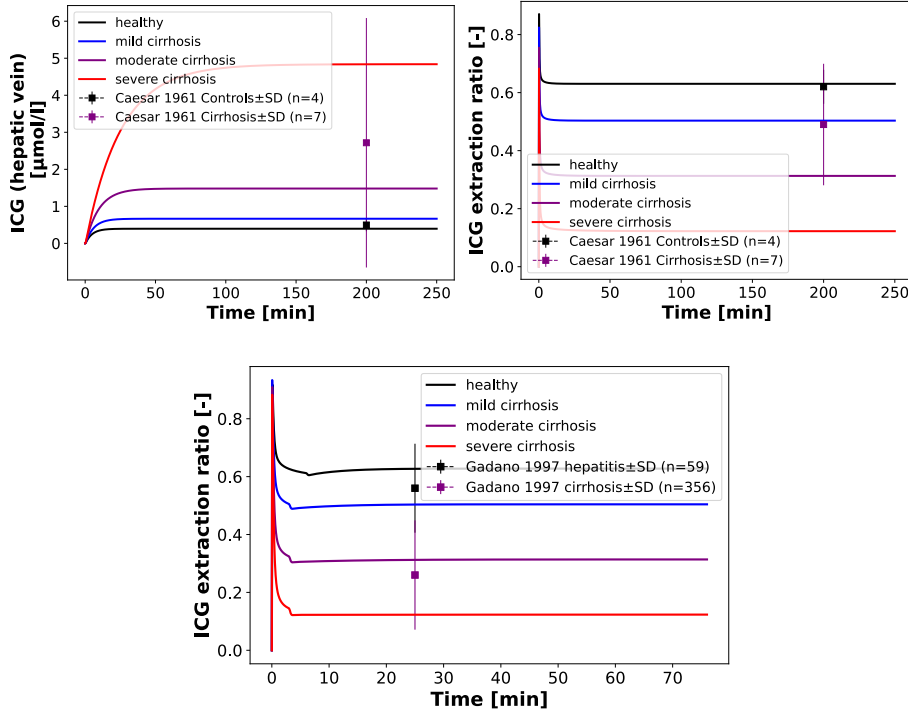


Figure 15: Simulation of hepatic venous and arterial ICG concentrations and ICG extraction-ratio in cirrhosis and healthy subjects compared to clinical data [8, 16].

Overall, the model prediction of the differences in hepatic venous ICG concentration and ICG extraction-ratio agrees well with the clinical data [8, 16]. Fig. 15 shows that concentrations of ICG are increased in cirrhosis, as the liver loses its ability to eliminate ICG from the blood. With increasing cirrhosis degree, the time it takes until the ICG plasma concentration has reached steady state increases. The ICG extraction-ratio is reduced in cirrhosis. The model prediction of the healthy liver agrees well with the clinical data. In addition, the data points of the cirrhotic subjects lie in between the model predictions for different cirrhosis degrees.

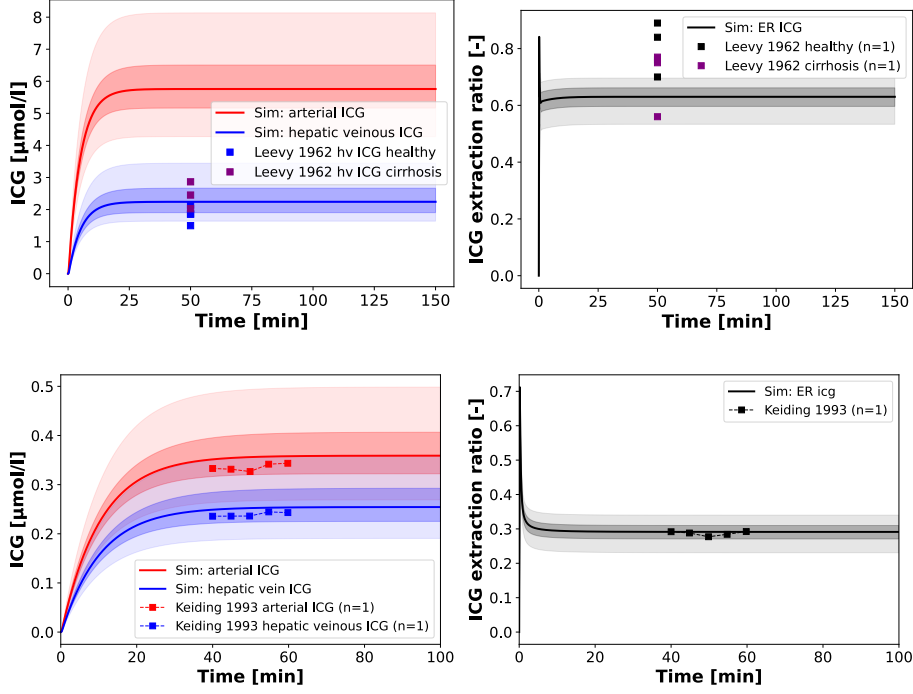


Figure 16: Simulation of hepatic venous and arterial ICG concentrations and ICG extraction-ratio in cirrhosis and in healthy subjects compared to clinical data [40, 35]. **Top:** Simulation of a healthy liver ($f_{cirrhosis} = 0$) with data of healthy and cirrhotic subjects. **Bottom:** Simulation of a cirrhotic liver with $f_{cirrhosis}$ set to 0.54.

Fig. 16 shows the differences in the clinical data between healthy and cirrhotic patients. Additionally, it shows the difficulty of accurately predicting both the ICG concentrations in the hepatic vein and artery at the same time as the extraction-ratio. When the hepatic venous ICG concentration is predicted accurately, the extraction-ratio is underestimated. Keiding et al. [35] measured the ICG extraction-ratio in a cirrhotic patient. By setting $f_{cirrhosis}$ to a value of 0.54 the model exactly predicts the extraction-ratio, but overestimates the hepatic venous and arterial concentrations. Overall, the model prediction agrees well with the clinical data.

Next, the correlation between different ICG pharmacokinetic parameters was studied and compared to published datasets that contain multiple ICG measurements for control subjects and cirrhotic patients [8, 9] (Fig. 17).

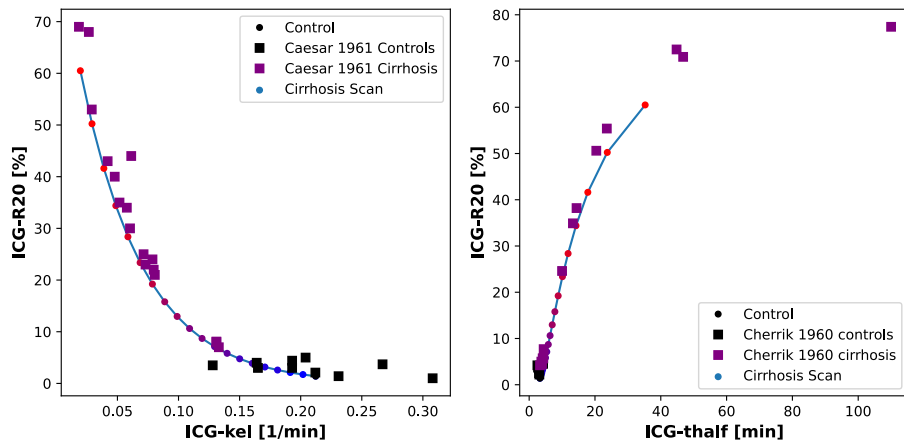


Figure 17: Simulation of correlation of ICG pharmacokinetic parameters in cirrhosis. The clinical data was published by Caesar et al. [8] and Cherrik et al. [9].

By varying the $f_{cirrhosis}$ parameter from 0 to 0.9 we can simulate different degrees of cirrhosis and predict the nonlinear relation between ICG-R20 and ICG-kel as well as ICG-R20 and ICG-t_{1/2}. As seen in the systematic analysis (Fig. 13) ICG-t_{1/2} and ICG-R20 are increased in cirrhosis and ICG-kel is reduced in cirrhosis. The same effect can be seen in the clinical data. As a result the relation between the ICG pharmacokinetic parameters is predicted accurately by the model.

Leevy et al. [41] compared the ICG-PDR in cirrhotic patients, acute and recovering hepatitis and control subjects after different doses of ICG (0.5 mg/kg and 5.0 mg/kg ICG). Burns et al. [6] compared the ICG-clearance after a bolus ICG administration and during a constant infusion in cirrhotic patients. The comparison of the clinical data with our model prediction is shown in Fig. 18.

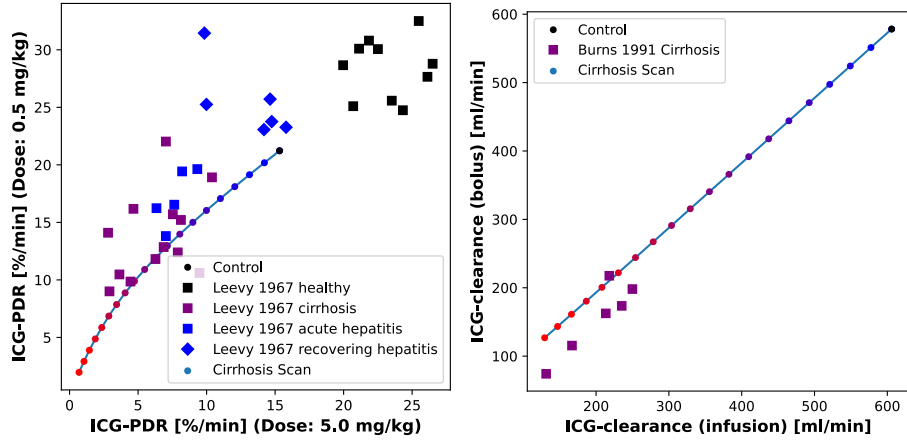


Figure 18: Simulation of ICG pharmacokinetic parameters in cirrhosis for different dosing/infusion protocols. **left:** Comparison of ICG-PDR after an ICG dose of 0.5 mg/kg and 5.0 mg/kg. Clinical data from Leevy et al. [41]; **right:** Comparison of ICG-clearance after a bolus ICG administration of 0.5 mg/kg and a constant infusion of 0.25 mg/min. Clinical data from Burns et al. [6]

The clinical data shows higher ICG-PDR values after an ICG dose of 0.5 mg/kg than after an ICG dose of 5.0 mg/kg. The model prediction agrees well with the clinical data. Interestingly, the ICG-PDR in acute and recovering hepatitis resembles that of mild to moderate cirrhosis. This is caused by inflammation and consequent loss of liver function. When comparing ICG-clearance after a bolus ICG administration and during a constant infusion, clinical data and model prediction both show good positive correlation. The model predicts a linear relationship that agrees well with the clinical data from Burns et al. [6].

As described in Sec. 1.6.1 the CTP-score is a scoring system that describes the severity of liver cirrhosis in a patient. In order to apply this model in a clinical setting, the model has to be adjusted individually according to the severity of cirrhosis in a patient. To see how the $f_{cirrhosis}$ parameter of the model relates to the CTP-Score we used datasets where ICG pharmacokinetic parameters were reported in patient groups of different CTP-Scores [15, 48, 49, 25].

First, a simulation was performed where ICG pharmacokinetic parameters were calculated for varying $f_{cirrhosis}$ values ranging from 0.0 to 0.9. Then the clinical values of the ICG pharmacokinetic parameters were plotted where they equal the model prediction. The corresponding $f_{cirrhosis}$ values were then compared between the different patient groups. Additional individual data from Figg et al. [15] is plotted. The results are shown in Fig. 19

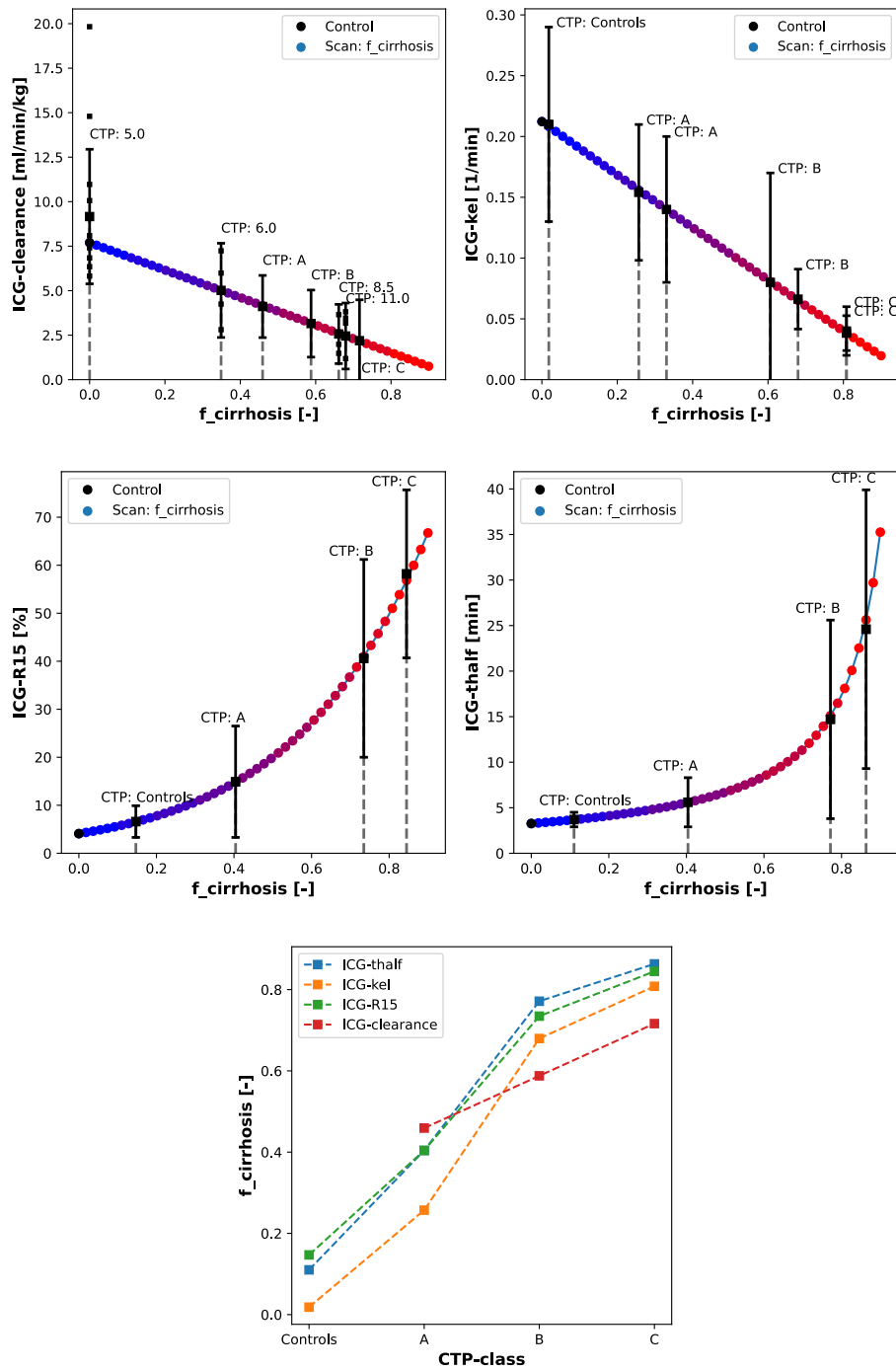


Figure 19: Mapping of the CTP-score on $f_{cirrhosis}$ using 4 different ICG pharmacokinetic parameters and data from 4 clinical studies [15, 25, 48, 49]

The results show a clear correlation between $f_{cirrhosis}$ and the CTP-classes

of the patient groups. The $f_{cirrhosis}$ values for the controls groups are close to 0, increasing with the CTP-class. The relation appears nonlinear, as the differences in $f_{cirrhosis}$ between CTP-B and CTP-C is smaller than between the control groups and CTP-A as well as CTP-A and CTP-B respectively. The mappings of CTP-class to $f_{cirrhosis}$ for the different ICG parameters give very similar results.

Unfortunately, only a single study reported the CTP-Score of the patient groups and they only reported ICG-clearance [15]. Other studies instead used the CTP-classes (A, B, C) [48, 49, 25]. With a large dataset of individually reported CTP-scores and ICG pharmacokinetic parameters of cirrhotic patients, it would be possible to calculate the relationship of the CTP-score on the $f_{cirrhosis}$ parameter more accurately. With a more accurate mapping the model could be adjusted for any individual subject suffering from liver cirrhosis. This would enable the model to individually predict ICG pharmacokinetics, if the subjects corresponding CTP-score is known.

3.5.2 Blood flow dependency

ICG-elimination is dependent on hepatic blood flow due to its high extraction ratio as described in Sec. 1.4. In order to simulate this dependency, the hepatic blood flow in our model was varied as described in Sec. 3.2.3.

We simulated the relative change in ICG-clearance during an intravenous infusion while varying the hepatic blood flow in a healthy liver (Fig. 20, top-left). Clearance during infusion was calculated as

$$Cl_{inf} = \frac{R_{inf}}{[ICG]_{\text{plasma}}} \quad (28)$$

where R_{inf} is the rate of infusion and $[ICG]_{\text{plasma}}$ is the plasma concentration of ICG during a steady state. The model prediction was compared to a dataset published by Kanstrup et al. [31].

Additionally, the dependency of ICG-clearance on hepatic blood flow in different degrees of cirrhosis was simulated (Fig. 20, top-right, bottom-left), and the effect of varying blood flow on the extraction-ratio of ICG in various degrees of cirrhosis was studied (Fig. 20, bottom-right).

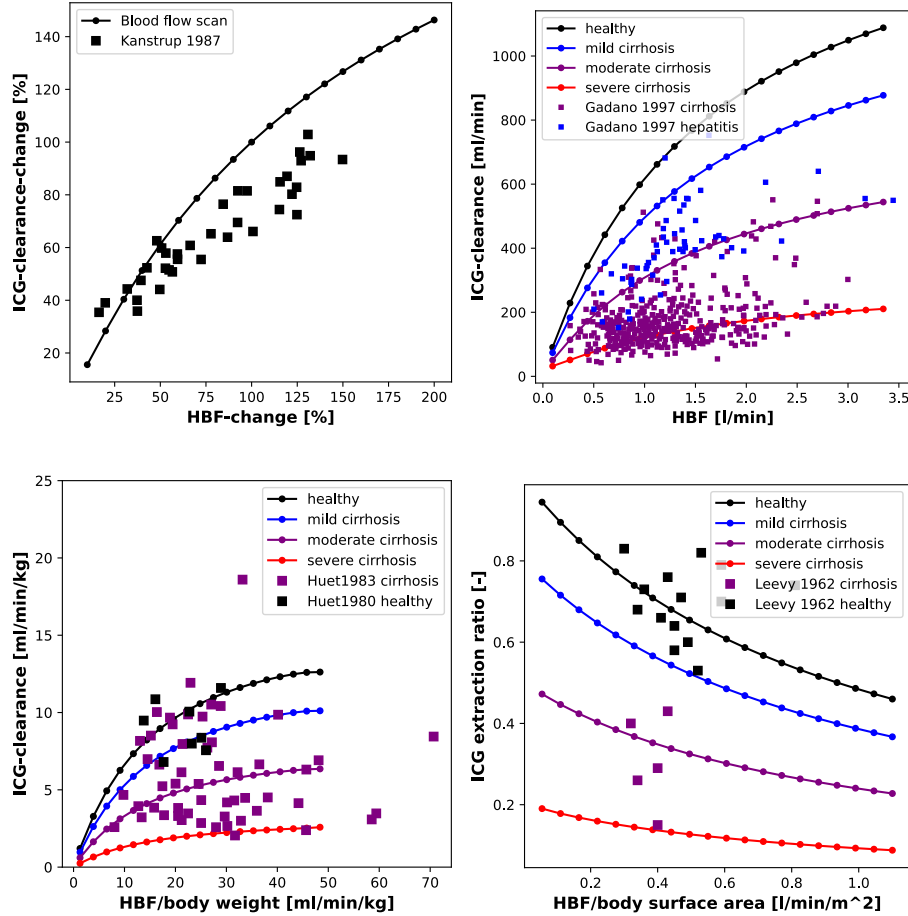


Figure 20: Dependency of ICG pharmacokinetics on hepatic blood flow. **top left:** Change in ICG-clearance by change in hepatic blood flow. Clinical data from Kanstrup et al. [31]; **top right:** Dependency of ICG-clearance during infusion on hepatic blood flow in hepatitis and cirrhosis. Clinical data from Gadano et al. [16]; **bottom left:** Dependency of ICG-clearance after bolus administration on hepatic blood flow. Clinical data from Huet et al. [28, 27]; **bottom right:** Dependency of ICG extraction-ratio on hepatic blood flow normalized to the body surface area in healthy subjects and in cirrhosis. Clinical data from Leevy et al. [40].

ICG-clearance increases nonlinearly with increasing hepatic blood flow and is highest in the healthy liver and lowest in the severely cirrhotic liver. However, ICG-clearance depends more strongly on hepatic blood flow in a healthy liver than in cirrhosis. This effect is caused by the shunts in the cirrhotic liver. They take a part of the liver blood supply and bypass it directly into the hepatic vein. As a result, reducing hepatic blood flow in a cirrhotic liver has less of an effect than in a healthy liver. The model prediction is in good agreement with experimental data [31, 16, 28, 27] both in cirrhotic patients and in healthy subjects and has similar variability to the experimental data through varying the degree of cirrhosis. Gadano et al. [16] measured hepatic blood and ICG-clearance in cirrhotic patients and in subjects with hepatitis B and C with

normal liver architecture. The patients with hepatitis are in good agreement with the model prediction of mild cirrhosis (see Fig. 20 (top-right)). In Fig. 20 (bottom left), the hepatic blood flow and ICG-clearance are both normalized to the body weight. As a result there are some data points that lie outside of the normal range of hepatic blood flow. This might be caused by variations in the body weight of patients with severe cirrhosis.

The extraction-ratio is calculated as described in Sec. 2.1. The hepatic blood flow was normalized to the body surface area in order to compare it to experimental data published by Leevy et al. [40]. The model prediction shows that the ICG extraction-ratio decreases with increasing hepatic blood flow. This is caused by the fact that the liver has less time to extract ICG from the blood as hepatic blood flow increases. As a result the difference in ICG plasma concentration between the hepatic vein and the portal vein or hepatic artery is lower, which is proportional to the extraction-ratio. Additionally, the extraction-ratio of ICG decreases with increasing degree of cirrhosis, because the amount of active parenchyma is decreased and a fraction of the liver blood supply is bypassed directly into the hepatic vein so no ICG is extracted from it.

Finally, a systematic analysis of ICG-pharmacokinetic parameters under varying blood flow for different degrees of cirrhosis was performed (Fig. 21).

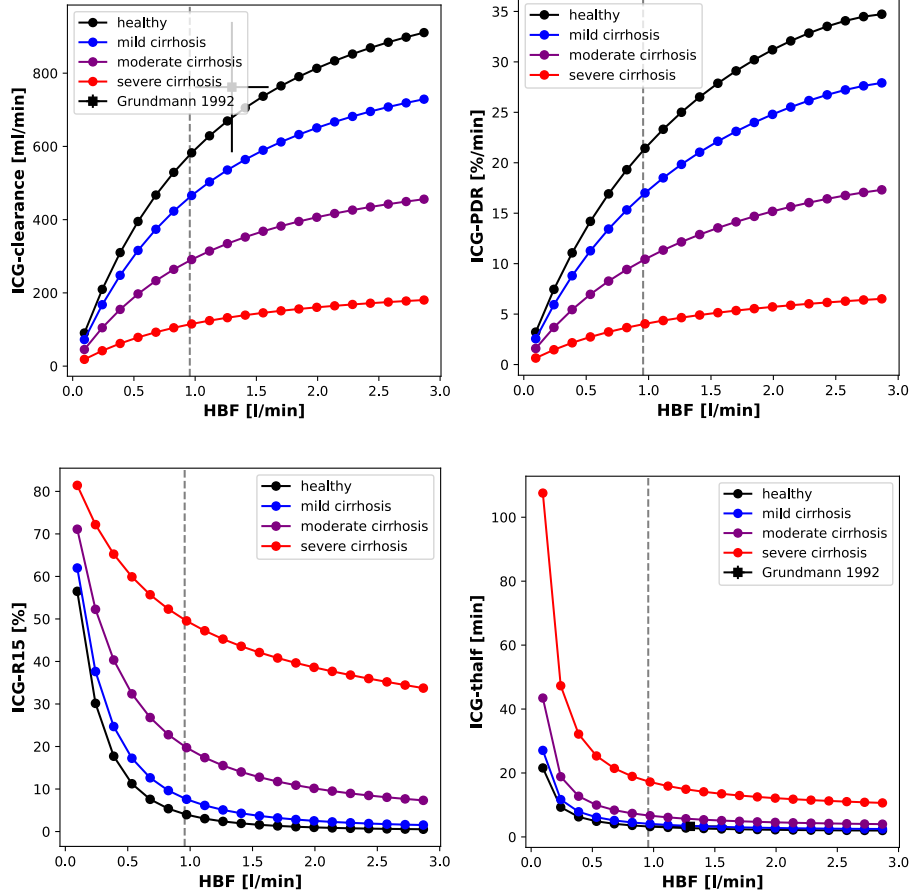


Figure 21: Dependency of ICG pharmacokinetic parameters on hepatic blood flow in four degrees of cirrhosis (**black** - healthy: $f_{cirrhosis}=0.0$; **blue** - mild cirrhosis: $f_{cirrhosis}=0.2$; **purple** - moderate cirrhosis: $f_{cirrhosis}=0.5$; **red** - severe cirrhosis: $f_{cirrhosis}=0.8$).

All ICG-pharmacokinetic parameters show a nonlinear dependency on hepatic blood flow. When hepatic blood flow is low, ICG pharmacokinetic parameters change strongly but as hepatic blood flow increases they converge toward a threshold value, that depends on the degree of cirrhosis. In contrast to other parameters, ICG- $t_{1/2}$ changes most strongly in the severely cirrhotic liver. For ICG-clearance and ICG- $t_{1/2}$ the model prediction was compared to clinical data published by Grundmann et al. [19]. They are in good agreement with each other.

In order to simulate changes in hepatic blood flow, a second approach was taken. Instead of only reducing the fraction of blood that flows through the liver, the cardiac output was reduced as described in Sec. 3.5.2. The effect of reducing cardiac output on ICG pharmacokinetic parameters was analyzed for different degrees of cirrhosis (Fig. 22).

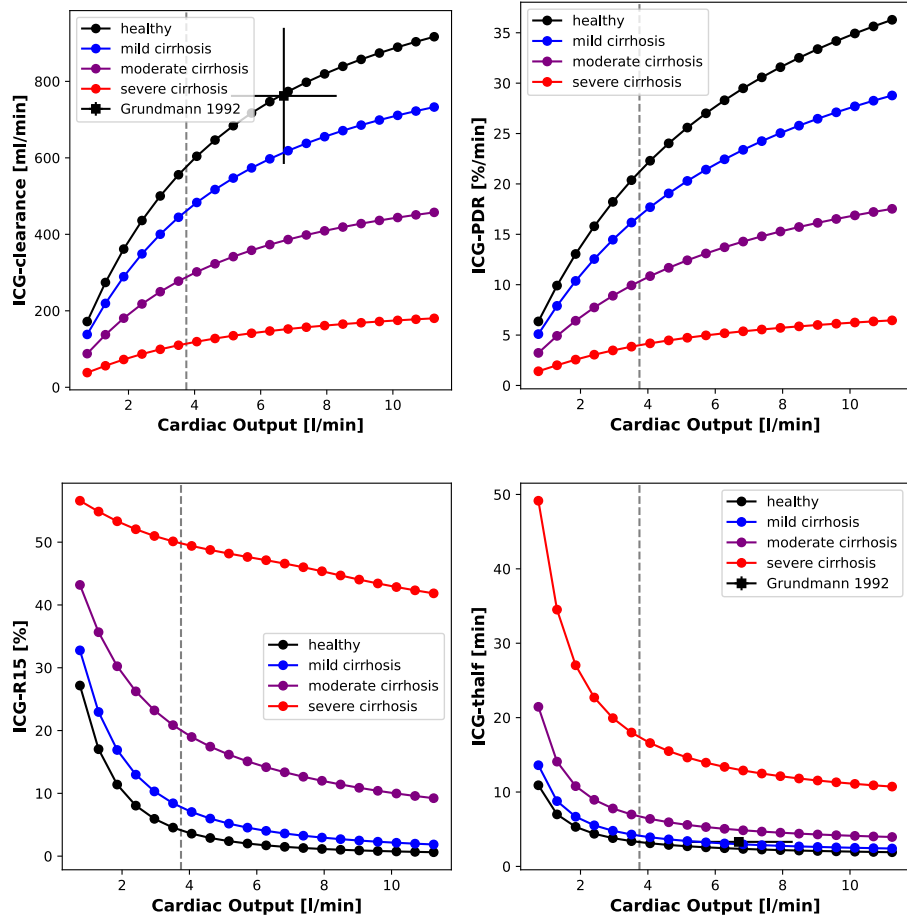


Figure 22: Dependency of ICG pharmacokinetic parameters on cardiac output in four degrees of cirrhosis (**black** - healthy: $f_{cirrhosis}=0.0$; **blue** - mild cirrhosis: $f_{cirrhosis}=0.2$; **purple** - moderate cirrhosis: $f_{cirrhosis}=0.5$; **red** - severe cirrhosis: $f_{cirrhosis}=0.8$).

When cardiac output is changed, ICG-clearance and ICG-PDR behave similarly to when only hepatic blood flow is changed. However, ICG-t_{1/2} is generally lower than it is when only reducing hepatic blood flow, most significantly in the severely cirrhotic liver. Additionally, ICG-R15 in the severely cirrhotic liver shows an irregularly linear dependency on cardiac output. For ICG-clearance and ICG-t_{1/2} the model prediction was compared to clinical data published by Grundmann et al. [19]. They are in good agreement with each other.

The dependency of ICG parameters on cardiac output is of clinical relevance and ICG parameters will most likely be altered in patients with heart insufficiencies.

3.5.3 Plasma proteins (bilirubin dependency)

As described in Sec. 1.5 ICG-elimination depends on plasma proteins. This dependency was implemented in the model via inhibition of ICG hepatic uptake by bilirubin as described in Sec. 3.2.5.

We simulated the dependency of different ICG pharmacokinetic parameters on the bilirubin plasma concentration in a healthy liver and three different degrees of cirrhosis (healthy: $f_{cirrhosis}=0.0$; mild cirrhosis: $f_{cirrhosis}=0.2$; moderate cirrhosis: $f_{cirrhosis}=0.5$; severe cirrhosis: $f_{cirrhosis}=0.8$) (Fig. 23).

ICG-clearance decreases nonlinearly with increasing bilirubin concentration and is lowest in the severely cirrhotic liver. The model prediction of ICG-clearance is in good agreement with clinical data published by Branch et al. [5] and Kawasaki et al. [32]. With increasing bilirubin concentration ICG-kel decreases, being lowest in the severely cirrhotic liver. The simulation results agree well with the clinical data from Caesar et al. [8] and D’Onofrio et al. [13]. The model accurately predicts the changes in ICG extraction-ratio when the plasma bilirubin concentration is varied (clinical data published by Leevy et al. and Caesar et al. [40, 8]). The simulated ICG-R20 and ICG-R15 values increase with increasing bilirubin plasma concentration and compare well to clinical data [8, 13].

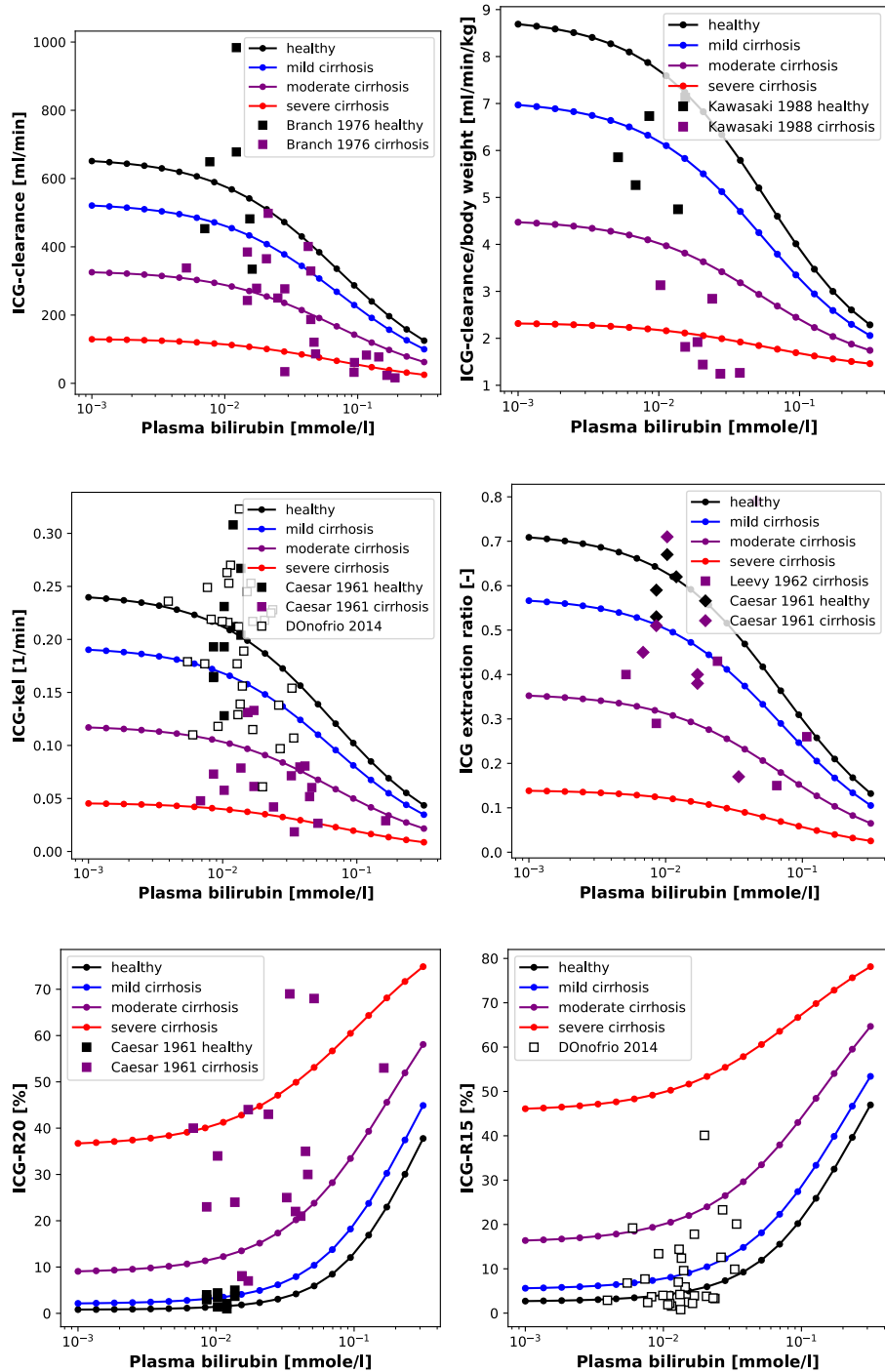


Figure 23: Model prediction of the dependency of ICG pharmacokinetic parameters on the plasma bilirubin concentration in a healthy liver and three different degrees of cirrhosis. The results are compared to clinical data of healthy subjects (black squares), cirrhotic patients (purple squares) and non-cirrhotic liver disease patients/other disease (white squares) [5, 32, 8, 13, 40].

Further, a systematic analysis of the bilirubin dependency of ICG pharmacokinetic parameters was performed (Fig 24).

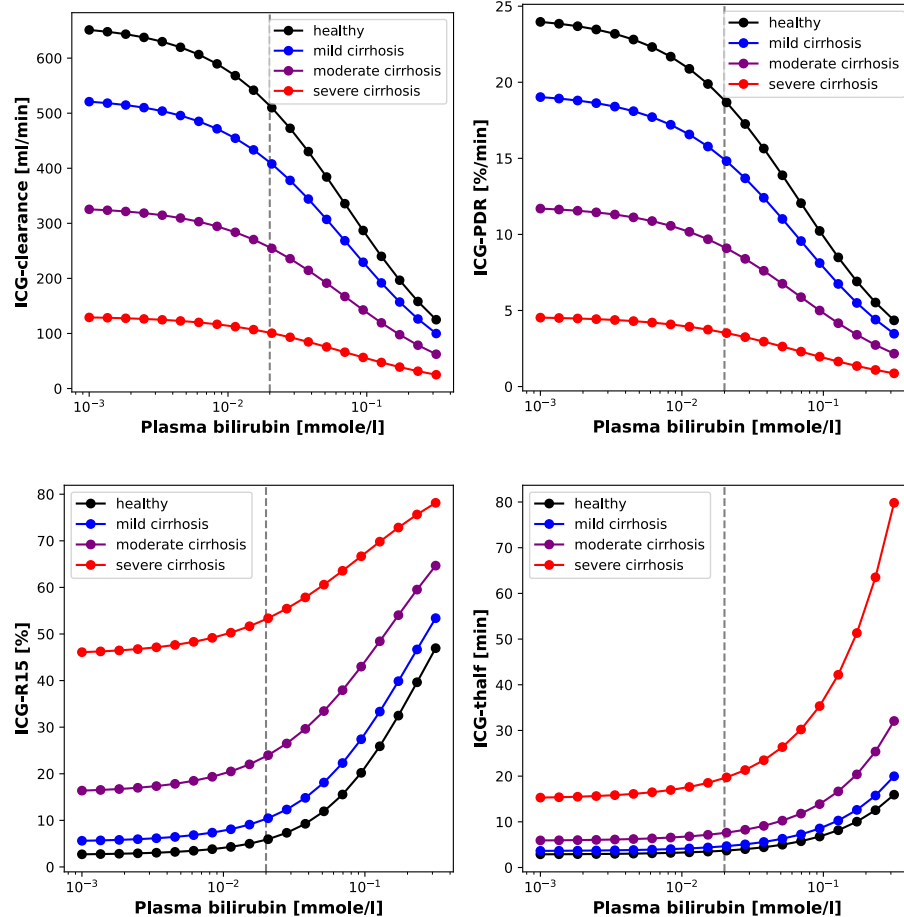


Figure 24: Systematic analysis of the effect of varying bilirubin plasma concentrations on ICG pharmacokinetic parameters. Model prediction for a healthy liver and three different degrees of cirrhosis (black - healthy: $f_{cirrhosis}=0.0$; blue - mild cirrhosis: $f_{cirrhosis}=0.2$; purple - moderate cirrhosis: $f_{cirrhosis}=0.5$; red - severe cirrhosis: $f_{cirrhosis}=0.8$)

The results show that the model is able to predict changes in ICG pharmacokinetics due to varying bilirubin plasma concentrations. Bilirubin is an important factor influencing ICG parameters and should be routinely measured in the clinics when performing ICG liver function tests.

3.5.4 Hepatectomy

Hepatectomy was simulated by removal of liver volume as described above (see 3.2.7) under varying severity of cirrhosis (healthy: $f_{cirrhosis}=0.0$; mild cirrhosis: $f_{cirrhosis}=0.2$; moderate cirrhosis: $f_{cirrhosis}=0.5$; severe cirrhosis:

$f_{cirrhosis}=0.8$) as described above (see 3.2.6).

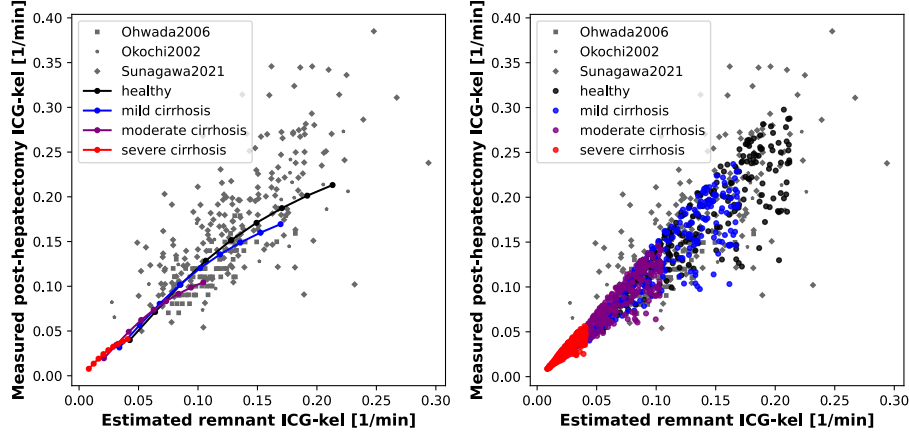


Figure 25: **Left:** Simulation of change of ICG-kel in hepatectomy. **Right:** Simulation of change of ICG-kel in hepatectomy with additional postoperative blood flow variability. Data from Ohwada et al. [52], Okochi et al. [53], Sunagawa et al. [69]

The correlation between measured post-hepatectomy ICG-kel and estimated remnant ICG-kel (described in Sec. 1.7) was simulated under various degrees of cirrhosis (Fig. 25). The model predictions were compared to three different data sets [52, 53, 69].

A good correlation between post-hepatectomy ICG-kel and estimated remnant ICG-kel (based on preoperative ICG-kel and predicted future liver remnant) can be observed. The model predictions are in good agreement with the experimental data. In addition, all data sets are in good agreement with each other.

The simulated correlation line is independent of the cirrhosis degree, but with increasing cirrhosis ICG-kel decreases. A large variability can be observed in the experimental data, but as our simulations indicate is most likely not due to cirrhosis.

Kawasaki et al. [33] evaluated the change in hepatic blood flow after resection and found no significant change towards increase or decrease, except when the resection rate was very high. However, their data shows that hepatic blood flow on an individual level can vary up to 50% after hepatectomy. Kin et al. [36] reported significant correlation between the postoperative growth rate of the liver and the postoperative mean portal velocity. To test if the variability could be due to post-operative changes in blood flow, an additional variability in hepatic blood flow was added to the simulation (equal distribution: $0.5-2 \cdot$ reference value) The resulting variability in predicted ICG-kel is comparable to the variability present in the experimental data (see Fig. 25 (right)). The individual variation in blood flow following hepatectomy could be a possible explanation for the large variability observed in post-hepatectomy ICG parameters.

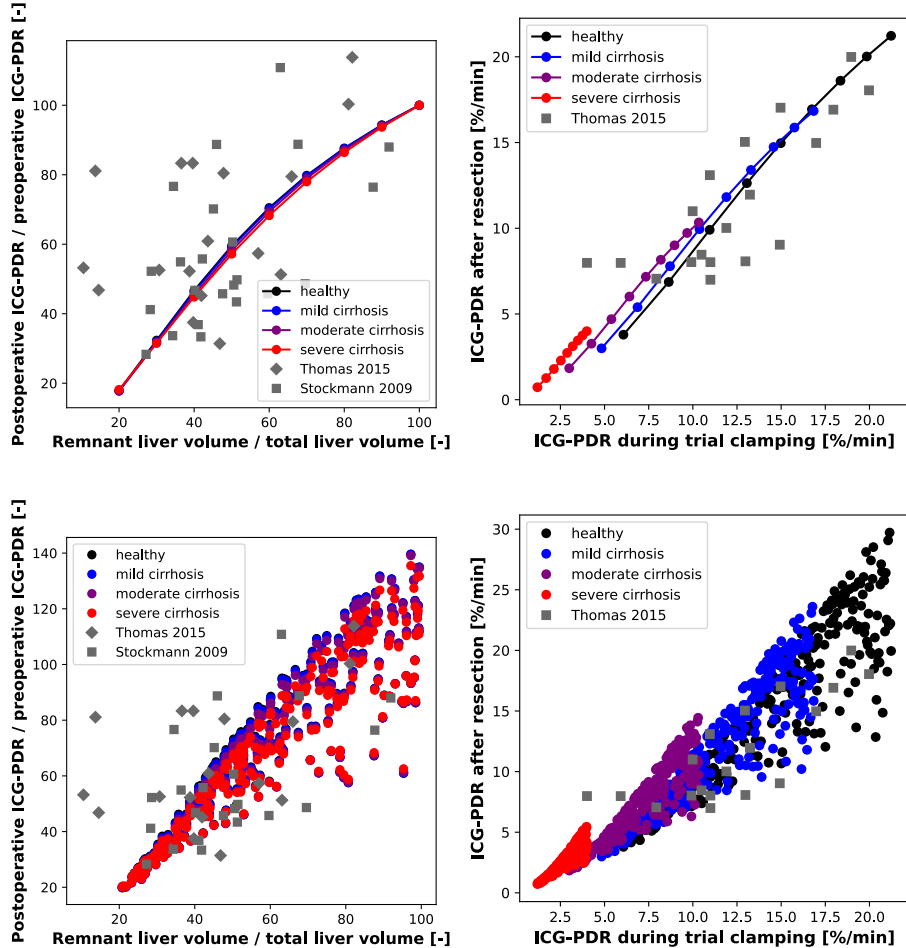


Figure 26: **Left:** Change in ICG-PDR compared to change in liver volume in hepatectomy. **Right:** Postoperative ICG-PDR compared to intraoperative ICG-PDR during trial-clamping. **Bottom:** Additional postoperative blood flow variability. Clinical data from Thomas 2015 [70] and Stockmann 2009 [68]

Further, we simulated the relative change in ICG-PDR as a function of the relative change in liver volume (Fig. 26 (left)). The model predicts a linear dependency of change in ICG-PDR with change in liver volume independent of the degree of cirrhosis. The model predictions are in agreement with the experimental data from Thomas et al. [70]. However, the model prediction did not achieve the same variability through variations in the cirrhosis degree alone. However, when blood flow variability is added postoperatively, similar variability is achieved.

Furthermore, the simulation shows no difference in the relative change of ICG-PDR between cirrhosis degrees.

As mentioned in 1.7, Thomas et al. found significant correlation between post-hepatectomy ICG-PDR and intraoperative ICG-PDR measured under trial clamping. This was simulated by changing hepatic blood flow and liver volume

in separate simulations but in the same intervals. This was performed for a healthy liver as well as three different degrees of cirrhosis (Fig. 26 (right)). The model prediction agrees very well with the experimental data and achieves similar variability when blood flow variation is added postoperatively.

In general, it seems that the prediction for a severely cirrhotic liver is not in good agreement with experimental data. This reflects that no resection would be conducted to a severely cirrhotic liver due to high risk of postoperative complications. So most of the hepatectomies are performed in mild to moderate cirrhosis.

To analyse the effect of hepatectomy on ICG pharmacokinetics we simulated the change in ICG pharmacokinetic parameters as a function of the fractional remnant liver volume (see Fig. 27). The scan was performed for a healthy liver as well as three different degrees of cirrhosis.

ICG-clearance and ICG-PDR are highest in the preoperative liver (total liver) and decreases with increasing hepatectomy whereas ICG- $t_{1/2}$ and ICG-R15 are lowest in the healthy liver and increase with increasing hepatectomy. ICG-clearance and ICG-PDR are highest in the healthy liver and decreases with increasing cirrhosis degree whereas ICG- $t_{1/2}$ and ICG-R15 are lowest in the healthy liver and increase with cirrhosis degree. The dependency of ICG pharmacokinetic parameters on hepatectomy increases with cirrhosis degree. Both hepatectomy and cirrhosis result in loss of functional liver volume resulting in an analogous change in ICG pharmacokinetic parameters.

The dependency of ICG-clearance, ICG-PDR and ICG-R15 on hepatectomy is almost linear, whereas the dependency of ICG- $t_{1/2}$ is highly non-linear. Furthermore, the dependency of ICG- $t_{1/2}$ on removed liver volume is marginal up until removal of 60% of liver tissue. The nonlinear dependency only arises for resection rates of over 60%.

Moreover, in the severely cirrhotic liver ICG- $t_{1/2}$ is the only parameter that is greatly affected by a change in liver volume. For all other parameters seen here, the healthy liver is affected most by a change in liver volume. As expected ICG-clearance and ICG-PDR increase with increasing remnant liver volume while ICG- $t_{1/2}$ and ICG-R15 decrease.

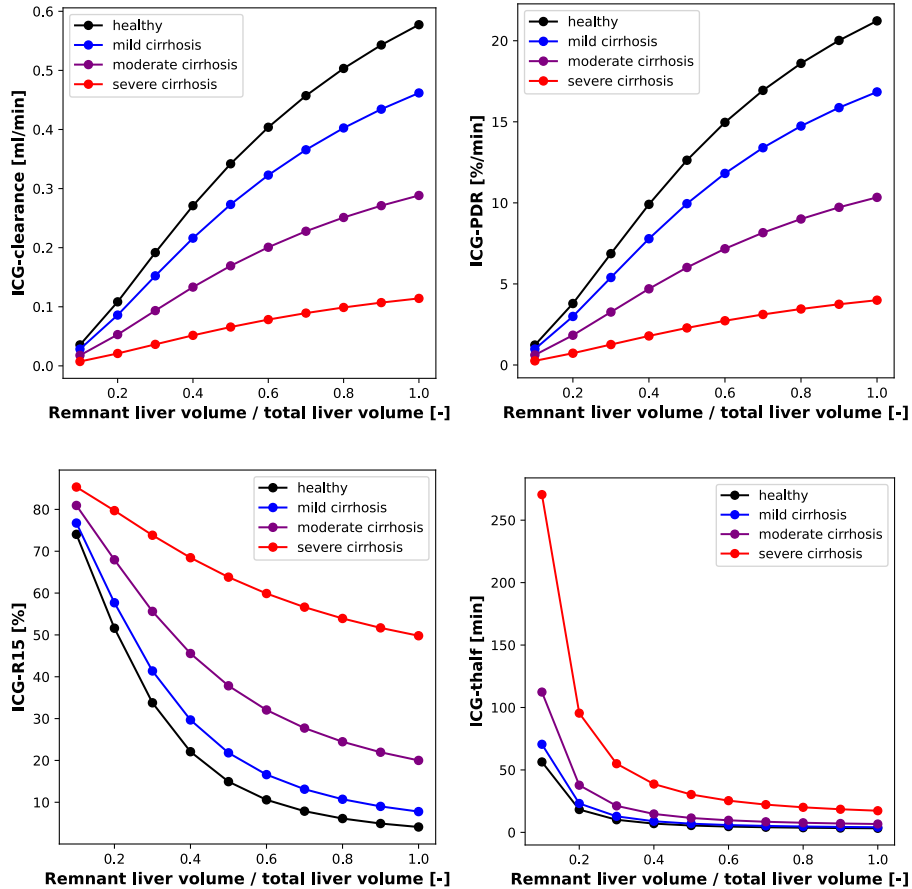


Figure 27: Effect of removal of different liver volumes on ICG pharmacokinetic parameters in four degrees of cirrhosis (black - healthy: $f_{cirrhosis}=0.0$; blue - mild cirrhosis: $f_{cirrhosis}=0.2$; purple - moderate cirrhosis: $f_{cirrhosis}=0.5$; red - severe cirrhosis: $f_{cirrhosis}=0.8$)

As shown here, the model allows to systematically predict the changes of ICG pharmacokinetic parameters in hepatectomy under various degrees of cirrhosis. Additionally, with the parameters that we were able to change in the model, we were successful in achieving similar variability to the experimental data for hepatectomy.

One possible clinical application of the presented model could be the prediction of survival for patients undergoing hepatectomy. ICG-R15 is often included in the decision process whether a patient is eligible for hepatectomy. As such, in clinical data preoperative ICG-R15 is often reported alongside the planned resection rate. As shown in Sec. 3.5.1 ICG-R15 depends heavily on the degree of cirrhosis. The model has shown to be able to accurately assess the relationship between cirrhosis and ICG-R15. By fitting the model parameter $f_{cirrhosis}$ as a function of its resulting ICG-R15 value to a logarithmic function $f_{cirrhosis} = a \cdot \ln(b \cdot x) + c$ where x is the ICG-R15 value, we are able to convert a clinically measured preoperative ICG-R15 value to a value of our model pa-

parameter $f_{cirrhosis}$, thereby providing an estimate of the cirrhosis degree. This information was used to predict the postoperative ICG-R15 of individual patients undergoing hepatectomy based on their preoperative ICG-R15 and the planned resection rate. The results are depicted in Fig. 28.

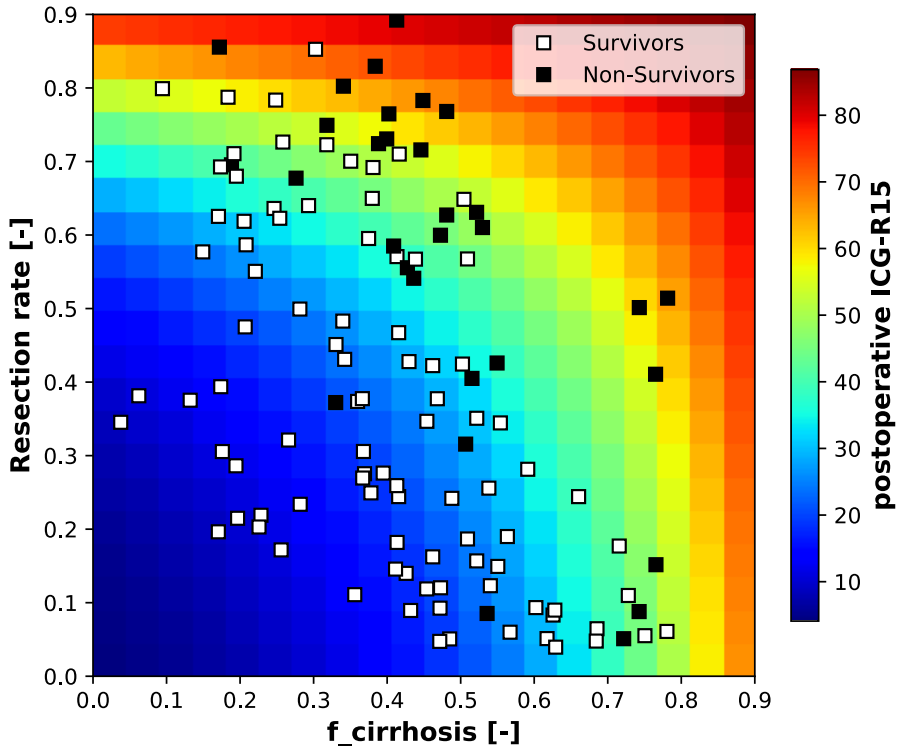
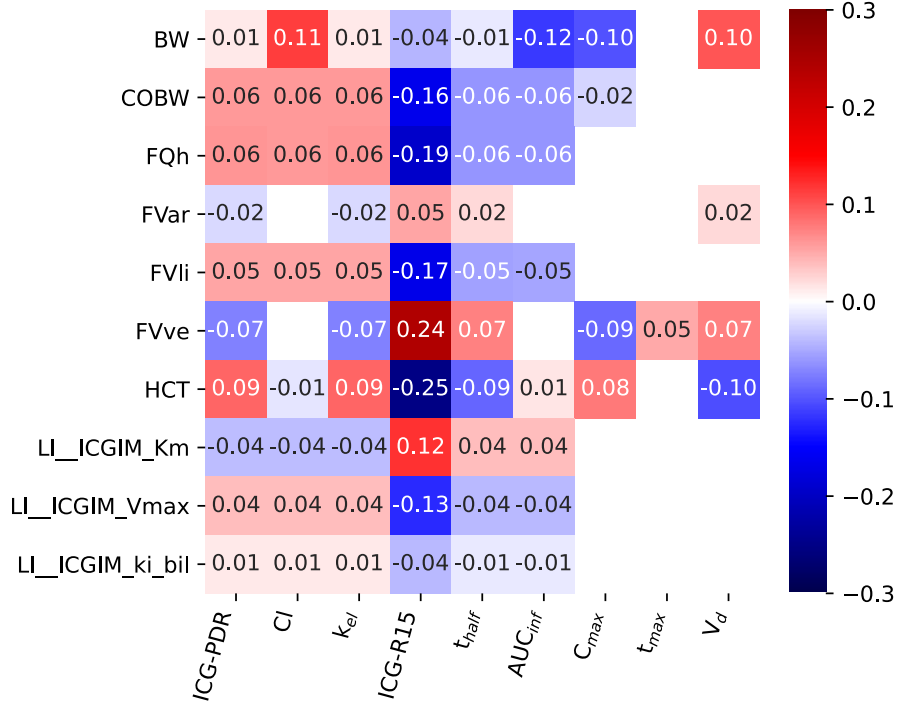


Figure 28: Heatmap showing the dependency of post-hepatectomy ICG-R15 on the degree of underlying cirrhosis and the planned resection rate. Clinical data published by Seyama et al. and Wakabayashi et al. [62, 74].

When clinical data from Seyama et al. and Wakabayashi et al. [62, 74] that differentiates survivors and non-survivors is added to the heatmap, a clear relationship between postoperative ICG-R15 and survival can be observed. With increasing cirrhosis degree and increasing resection rate the risk of not surviving the operation increases. Moreover, the model can be used as a decision-making tool, as it takes into account the underlying cirrhosis of a patient and can evaluate if the planned resection rate poses a risk of postoperative complications or mortality.

3.6 Sensitivity analysis

A systematic analysis of the effect of various model parameters on ICG pharmacokinetic parameters was performed as described in Sec. 2.6. Fig 29 shows the effect that each parameter has on different ICG pharmacokinetic parameters for typical ICG liver function test using an ICG dose of 0.5 mg/kg body weight.



BW :	Body weight
COBW :	Cardiac output per bodyweight
FQh :	Blood flow liver venous side
FVar :	Volume arterial blood
FVli :	Volume liver
FVve :	Volume venous blood
HCT :	Hematocrit
LI_ICGIM_Km :	Liver import km (icg)
LI_ICGIM_Vmax :	Liver import vmax (icg)
LI_ICGIM_ki_bil :	Inhibition constant of bilirubin

Figure 29: Systematic sensitivity analysis.

Because the body weights main effect is increasing organ and blood volumes in the model, it has a strong effect on the ICG-clearance, the area under the curve and the C_{max} value. The ICG-PDR and ICG- $t_{1/2}$, which are both derived from the ICG-kel are not changed, because the elimination rate is not affected by the body weight. $COBW$ is the parameter that determines the cardiac output in the model, and as a result has a strong effect in line with our cardiac output scans (Fig. 22). The fractional liver blood flow f_{Qh} (FQh) has a similar effect to the $COBW$ in line with our bloodflow scans (Fig. 21). The fractional liver volume $FVli$ determines the volume of the liver. Because the hepatic uptake kinetic scales with the liver volume, the livers capacity to eliminate ICG increases with the $FVli$. Alteration of liver volume can have a strong effect on

ICG parameters in line with our hepatectomy scans (Fig. 27). $FVve$ is the volume of the venous blood and therefore directly affects the ICG venous plasma concentration. Because hepatic uptake depends on the ICG plasma concentration, elimination of ICG is reduced when $FVve$ is increased. The hematocrit HCT shows the inverse effect. With increasing hematocrit the plasma volume is decreased. The V_{max} and K_m parameters of the hepatic uptake affect ICG pharmacokinetic parameters in an opposite manner. This effect could also be observed during the parameter fitting of the model. When fitting the model parameters, the V_{max} and K_m of the hepatic uptake can change in orders of magnitude, for as long as they both change the same way, because they affect ICG pharmacokinetics in opposite directions. The inhibition constant of bilirubin has a small effect on ICG pharmacokinetics.

3.6.1 Protein dependency

In 2011 de Graaf et al. reported that ICG is mainly taken up into the liver by the organic anion transporting polypeptide 1B3 (OATP1B3) [12]. The individual ICG elimination capacity of any subject depends on the amount of OATP1B3 in its liver. Burt et al. showed that the distribution of this protein amount in the population resembles a lognormal distribution [7]. Throughout this project a key challenge was the large intra-individual variability in reported ICG data. A possible solution of predicting this variability with our model is by sampling the V_{max} of the hepatic uptake, which corresponds to the protein amount in a subjects liver, along a lognormal distribution. This simulation was compared to a large dataset published by Sakka et al. [61]. Additionally, variability in body weight was added to the simulation. In Fig. 30 the correlation of ICG-clearance and ICG-PDR is shown.

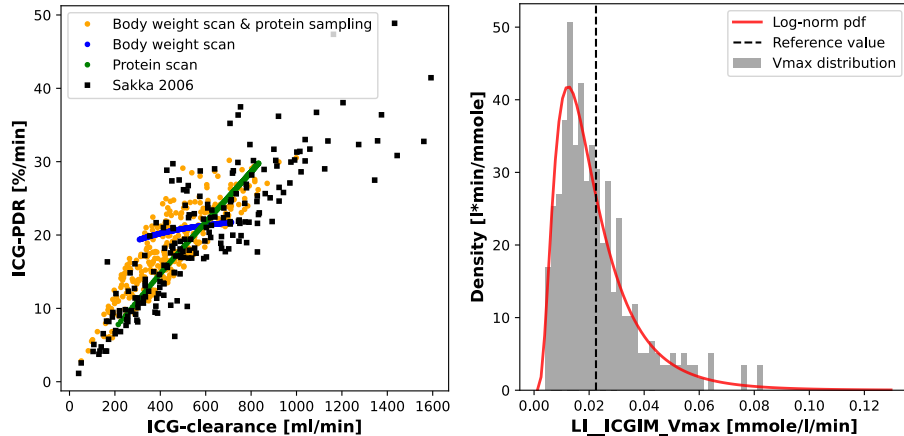


Figure 30: **left:** Correlation between ICG-clearance and ICG-PDR under sampling of protein amount along a lognormal distribution (yellow). Additionally a protein scan (green) and a body weight scan (blue) were performed, showing their individual effect on ICG-clearance and ICG-PDR. The clinical data was published by Sakka et al. [61]; **right:** The distribution that was used for the protein sampling (grey), with the probability density function of the lognormal distribution (red) and the reference V_{max} value.

With this approach we are able to predict variability that closely resembles that of the clinical data, showing that individual bodyweight and enzyme amount of OATP1B3 are important factors for predicting ICG pharmacokinetic parameters. The sampling of the protein amount varies ICG-clearance and ICG-PDR equally, whereas the variation of the body weight has a much stronger effect on ICG-clearance. For a more accurate prediction of ICG parameters, the protein amount of an individual subject would be an important parameter to include.

4 Discussion

4.1 Data

An important step of the project was to establish a database of ICG pharmacokinetic measurements from 36 clinical studies. The data presented in these studies showed strong heterogeneity in regard to their reporting of ICG pharmacokinetics and information on subjects (blood flow, bilirubin levels, etc.).

Whereas ICG parameters are often reported as part of studies, ICG time courses are only rarely reported. We were able to find only a small set of ICG time course data, which often were from single subjects (showing a representative time course), with only a few mean ICG time courses existing in the literature. This lack of reporting of available data was a major challenge for the project.

The subset of pharmacokinetic parameters that were reported varied as well. Only a few studies provided all relevant parameters (ICG-clearance, ICG-PDR, ICG-R15, ICG- $t_{1/2}$), whereas often only a single parameter was reported. The curated data comes from studies as old as 60 years as well as from the year 2020. Unfortunately, there is no established standard of publishing ICG pharmacokinetic data. Moreover, as Tab. 2 shows, there is no established standard for ICG administration protocols. Although a bolus dose of 0.5 mg/kg is most common, some deviations are observed. For ICG infusions, there is no standard infusion rate. This is a major issue for physiological-based modeling, because collecting literature data to support and validate a model is a crucial step in the modeling process.

In addition to the heterogeneity in the way the data is presented, large variability exists in the data itself, mainly due to interindividual variability in ICG elimination. The developed model is able to predict similar variability in ICG pharmacokinetics by varying parameters like body weight, hepatic blood flow and protein amount of the hepatic ICG transporter. However, more research is necessary into what the exact cause of this variability is. Importantly, most parameters resulting in large variability can be readily quantified in the clinical setting and could be used to improve the accuracy of the model predictions. Unfortunately, no high quality dataset was available reporting individual ICG time courses and pharmacokinetic parameters in combination with blood flow, anthropometric factors or plasma proteins.

4.2 Physiological-based modeling

The model which was developed in this project is based on the physiology of the human body and the pharmacokinetics of ICG. Although it is the objective of physiological-based modeling to approximate reality as accurately as possible, modeling ICG pharmacokinetics to its last detail is not possible. On the contrary, being able to reduce complex systems down to an abstract model is one of the key advantages of physiological-based modeling. We are able to predict ICG pharmacokinetics accurately with only a small set of parameters and processes. As a result the effect of these parameters on ICG pharmacokinetics can be studied. Key model simplifications were among others: (i) The underlying parameters such as organ volumes and blood flows of the model correspond to a reference male subject of 75 kg bodyweight. No changes in the underlying

physiology were simulated besides adjustment in bodyweight.; (ii) all other organs besides the lung, liver and gastrointestinal tract were pooled in a single rest compartment with a single overall perfusion. In reality these organs have different perfusion (slow and fast perfusing organs); (iii) plasma proteins were not modeled explicitly and no protein dependent uptake was included; (iv) The main focus of the model was a good description of the first 15-30 min after ICG application (used for calculation of ICG parameters). A slow second phase can be observed in the plasma ICG elimination at longer time intervals, but was not included in the model; (v) No delays were included in describing the blood flow. This results in instantaneous changes between blood compartments, whereas in reality delays occur between organs.

Despite these model simplifications and assumptions, the resulting model was able to correctly describe a large data base of heterogeneous data with various administration protocols. Although only a small subset of data was used for model parameterization (time course data), the large majority of the data could be predicted by the model and functions as validation of the model.

One exception should be noted here: In Fig. 11 the biliary excretion of ICG after three different doses was simulated. The clinical data shows a nonlinear dependency of the peak in the biliary excretion rate on the administered ICG dose. The model is not able to replicate this nonlinearity, but instead shows a linear relation between the peak in the biliary excretion and the ICG dose. This is the result of the simplification of the biliary excretion mechanism. To be able to predict this dependency accurately more information on the biliary excretion ICG would be required, as well as more time course data.

4.3 Bilirubin

As described in Sec. 3.2.5 we implemented the effect of the plasma protein binding of ICG in form of a competitive inhibition of ICG hepatic uptake by bilirubin. As shown in Sec. 3.5.3 we are able to accurately predict the dependency of ICG pharmacokinetics on the plasma concentration of bilirubin. We assumed the following mechanism of interaction between ICG and bilirubin: ICG and bilirubin both bind to the same plasma protein. For bilirubin to inhibit ICG hepatic uptake we had to assume a protein mediated uptake mechanism where the binding protein of ICG induces the hepatic uptake of ICG. Only then would a competitor for the protein binding sites inhibit ICG uptake by increasing its free fraction.

We were unable to find conclusive information about the protein binding of ICG and its effect on ICG pharmacokinetics (see Sec. 1.5). Therefore we chose to reduce the problem to a competitive inhibition of ICG elimination by bilirubin, without going in the mechanistic details underlying the inhibition. If more information were available on the plasma protein binding of ICG and the impact it has on ICG-elimination, the effect of bilirubin on ICG pharmacokinetics could be modeled more accurately.

When comparing the model prediction of the bilirubin dependency of ICG pharmacokinetics to clinical data, we are able to simulate underlying liver cirrhosis as well. However, changes in bilirubin can be caused by various diseases. The implementation of other diseases like Gilbert's disease and their effects on ICG pharmacokinetics into the model would be an interesting extension.

4.4 Blood flow

As described in Sec. 3.5.2 ICG pharmacokinetics depends strongly on blood flow. In the process of fitting the model parameters, a compromise between accurately predicting the ICG extraction ratio or accurately prediction the ICG plasma disappearance curves had to be found. Because the plasma disappearance curve of ICG is directly influenced by the extraction ratio one might expect we would be able to accurately predict both of them at the same time. However, due to way the extraction ratio is calculated, it can be influenced by certain parameters that have a different effect on the plasma disappearance curve. Specifically, this is the blood flow. To better understand this some theoretical considerations have to be made. The plasma disappearance curve is measured in the venous blood compartment. The extraction ratio is calculated from the difference in ICG concentration between the plasma that enters the liver and the plasma that leaves the liver. This difference is mainly affected by (i) the livers ability to eliminate ICG from the blood, (ii) the time it takes for the plasma that leaves the liver to complete a full circulation and enter the liver again. In an extreme example, where the blood that leaves the liver enters the liver again only one time step later, the difference between their ICG concentrations would be marginal. However, the plasma disappearance curve would not show any irregularities, as the ICG concentration still decreases with the same rate. As a result, the right amount of delay in the models circulation is crucial. This was achieved by reducing the cardiac output parameter of the model to a value at the lower end of its physiological range (3.75 l/min), which yielded the desired effect. An extension of the model with actual blood flow delays would allow to describe the data more accurately (e.g. using delay differential equations or a series of compartments to introduce the delay).

4.5 Hepatectomy

We have shown that the presented model accurately predicts changes in ICG pharmacokinetics after hepatectomy. It allows to include important factors that influence ICG pharmacokinetic parameters into the prediction. Importantly, the model allowed to predict survival status after hepatectomy using retrospective clinical data.

To apply this model clinically, a strategy would have to be developed for adjusting its parameters according to the physiology of an individual subject. This would ideally involve determining the subjects liver volume (e.g. via CT), their plasma protein and bilirubin levels (via plasma biochemistry), their cardiovascular parameters (cardiac output, hepatic blood flow, portal resistance, etc.), their transport protein amount (e.g. via liver biopsy), genetic variants that could affect ICG pharmacokinetics (e.g. of the OATP1B3 transporter [7]) or underlying liver disease. With this information and a model that can be adjusted accordingly more accurate predictions of postoperative outcome could be made. As a result, this model could become a valuable clinical tool used in the planning of liver resections.

In Sec. 3.5.4 we showed how ICG pharmacokinetics are affected by hepatectomy. Hepatectomy was simulated as a decrease in liver volume. However, the aftermath of such a highly invasive surgery is much more complex than can be described by this model. The liver is involved in the synthesis of lipoproteins,

albumin and bilirubin. As a result removing a part of the liver tissue affects the metabolism of these compounds. As ICG pharmacokinetics are influenced by the plasma protein binding, the effect of liver surgery on ICG pharmacokinetic becomes more unpredictable. Additionally, hepatic blood flow varies after hepatectomy [33] affecting ICG pharmacokinetics. In general, because blood flow is one of the most important factors for ICG pharmacokinetics, there should always be an accompanying hepatic blood flow measurement to any ICG measurement. Of course this measurement would have to be independent of ICG (e.g. via doppler ultrasound).

4.6 Disease

The conversion from CTP-score to the model parameter $f_{cirrhosis}$ yielded good results. As already mentioned in Sec. 3.5.1, to quantify this relation a large dataset of individually reported ICG measurements and CTP-scores would be necessary. However, the CTP-score takes into account bilirubin and albumin levels of a patient which would already be implemented in the model. As a result, if a patients high CTP-score is mainly caused by their bilirubin and albumin levels, the conversion to $f_{cirrhosis}$ would be biased. The CPT score is an overall score for the evaluation of liver status. The advantage that the presented model provides is being able to make a more differentiated evaluation of liver function.

Despite the very simplified description of cirrhosis (tissue loss and portal shunts) a wide range of ICG data could be correctly predicted in cirrhotic patients. Cirrhosis is a much more heterogeneous disease often accompanied by additional complications and alterations such as fibrosis, ascites or portal hypertension as well as comorbidities (e.g. diabetes, adipositas, liver cancer). A more detailed model of the changes in cirrhosis could further improve the predictive value of our model.

In this project we focused on cirrhosis as the prime example of liver disease because it is the end-stage of most other liver diseases. Being able to implement the effects of other diseases on ICG pharmacokinetics would be of high interest. This includes non-liver disease (e.g. cardiovascular disease) in addition to diseases that specifically change bile flow or bile excretion (e.g. primary biliary cholangitis).

5 Outlook

Individualization of physiology For this model to be applied in a clinical setting in the future, a process of adjusting the model parameters according to a subjects individual physiology has to be developed. The individualization of the model would include general information such as age, sex and ethnicity. Physiological information such as body weight, body fat percentage, cardiovascular parameters and organ volumes would be included. Additionally, plasma protein and bilirubin levels would need to be evaluated. Information regarding the liver specifically would be of the highest relevance. This includes liver perfusion, liver volume and transport protein amounts as well as assessment of possible underlying liver disease. A standard clinical protocol for acquiring the necessary information on the subject should be established.

Clinical validation Going forward, an important step would be to evaluate the model in the clinical context using a high quality dataset reporting individual ICG time courses in combination with all of the above-mentioned information about the subjects. This would allow to quantify the individual variability as well as the causing factors behind it more precisely.

A major achievement of the model presented here is the prediction of survival status after hepatectomy using retrospective clinical data. The model predictions would be evaluated based on another independent clinical dataset or more ideally in a prospective clinical trial. In this regard, validation with a dataset consisting of Caucasian subjects would be highly relevant, as the available survival data was based on hepatectomies in Japanese subjects.

Acknowledgements

I thank Dr. Matthias König for making this project possible. His experience in physiological-based pharmacokinetic modeling guided this project and his programming expertise was a reliable and oftentimes critical resource. Through him I was able to gain insight into the field of computational modeling of liver metabolism and acquire experience in physiological-based modeling. I thank Jan Grzegorzewski for his support in the data curation process. I also thank Florian Bartsch for our debates about this project and for his company during the online coffee breaks. I am grateful that I was able to work as a part of the research group Systems Medicine of the liver and take this first step into the world of scientific research.

6 Supplement

6.1 Dose dependency

Dose dependency of ICG pharmacokinetic parameters:

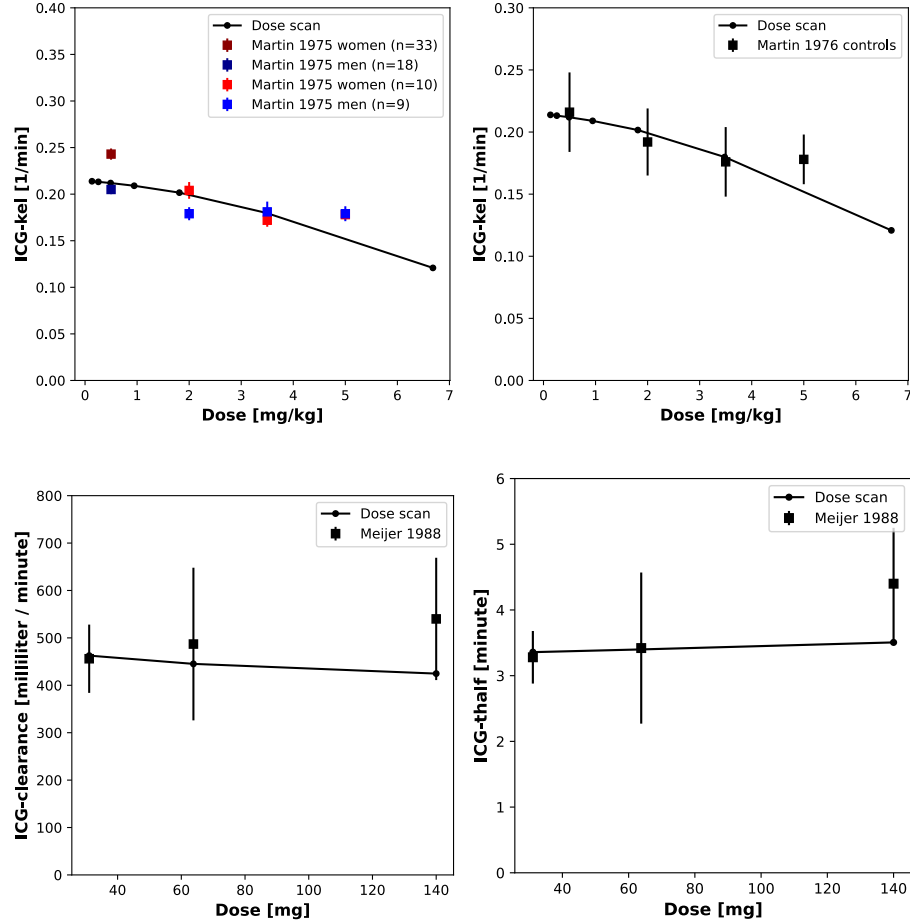


Figure 31: Simulation of dose-dependency compared to clinical data from [44, 45, 46]

Systematic analysis of the dependency of ICG pharmacokinetic parameters on the administered ICG dose.

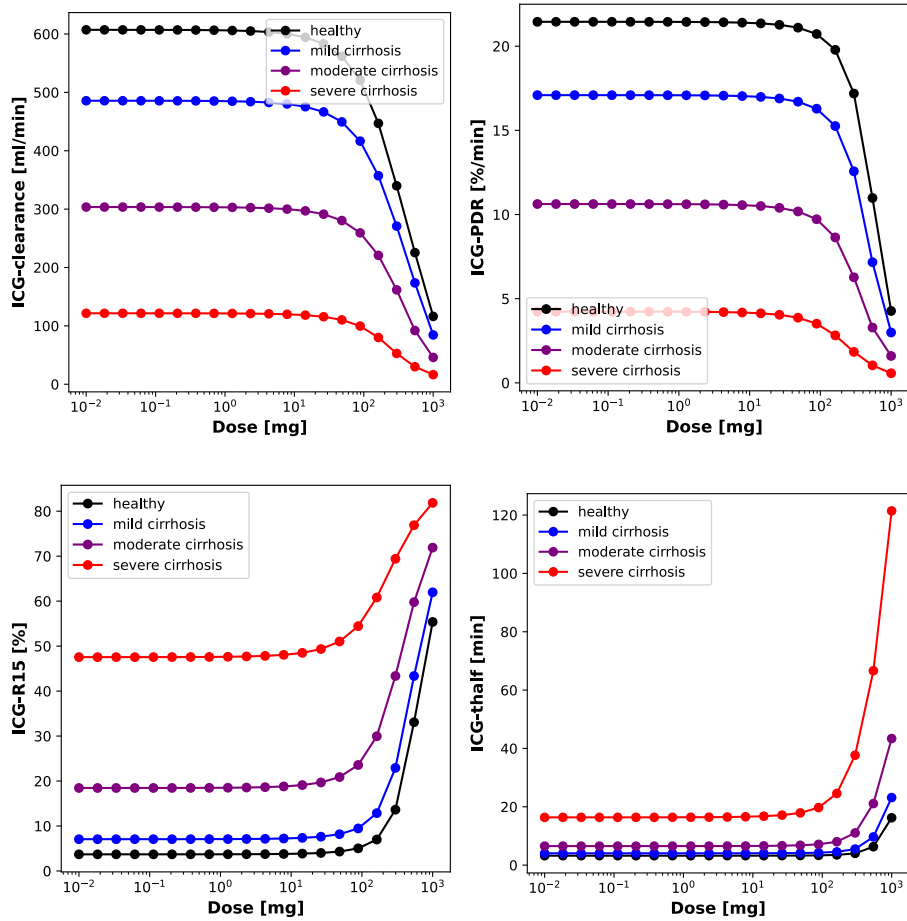


Figure 32: Systematic analysis of the dependency of ICG pharmacokinetic parameters on the administered ICG dose in the model prediction.

6.2 Model

The model can be accessed at <https://github.com/adriankl/icgmodel>.

References

- [1] V. Andersen, J. Sonne, and S. Larsen. Antipyrine, oxazepam, and indocyanine green clearance in patients with chronic pancreatitis and healthy subjects. *Scandinavian journal of gastroenterology*, 34:813–817, Aug. 1999.
- [2] K. J. Baker. Binding of sulfobromophthalein (bsp) sodium and indocyanine green (icg) by plasma alpha-1 lipoproteins. *Proceedings of the Society for Experimental Biology and Medicine. Society for Experimental Biology and Medicine (New York, N.Y.)*, 122:957–963, 1966.
- [3] P. D. Berk, B. J. Potter, and W. Stremmel. Role of plasma membrane ligand-binding proteins in the hepatocellular uptake of albumin-bound organic anions. *Hepatology (Baltimore, Md.)*, 7:165–176, 1987.
- [4] D. Birkett. *Pocket guide : pharmacokinetics made easy*. McGraw-Hill Australia, North Ryde, N.S.W, 2010.
- [5] R. A. Branch, J. A. James, and A. E. Read. The clearance of antipyrine and indocyanine green in normal subjects and in patients with chronic liver disease. *Clinical pharmacology and therapeutics*, 20:81–89, July 1976.
- [6] E. Burns, D. R. Triger, G. T. Tucker, and N. D. Bax. Indocyanine green elimination in patients with liver disease and in normal subjects. *Clinical science (London, England : 1979)*, 80:155–160, Feb. 1991.
- [7] H. J. Burt, A. E. Riedmaier, M. D. Harwood, H. K. Crewe, K. L. Gill, and S. Neuhoff. Abundance of hepatic transporters in caucasians: A meta-analysis. *Drug metabolism and disposition: the biological fate of chemicals*, 44:1550–1561, Oct. 2016.
- [8] J. Caesar, S. Shaldon, L. Chiandussi, L. Guevara, and S. Sherlock. The use of indocyanine green in the measurement of hepatic blood flow and as a test of hepatic function. *Clinical science*, 21:43–57, Aug. 1961.
- [9] G. R. Cherrick, S. W. Stein, C. M. Leevy, and C. S. Davidson. Indocyanine green: observations on its physical properties, plasma decay, and hepatic extraction. *The Journal of clinical investigation*, 39:592–600, Apr. 1960.
- [10] K. Chijiwa, M. Watanabe, K. Nakano, H. Noshiro, and M. Tanaka. Biliary indocyanine green excretion as a predictor of hepatic adenosine triphosphate levels in patients with obstructive jaundice. *American journal of surgery*, 179:161–166, Feb. 2000.
- [11] P.-A. Clavien, H. Petrowsky, M. L. DeOliveira, and R. Graf. Strategies for safer liver surgery and partial liver transplantation. *The New England journal of medicine*, 356:1545–1559, Apr. 2007.
- [12] W. de Graaf, S. Häusler, M. Heger, T. M. van Ginhoven, G. van Cappellen, R. J. Bennink, G. A. Kullak-Ublick, R. Hesselmann, T. M. van Gulik, and B. Stieger. Transporters involved in the hepatic uptake of (99m)tc-mebrofenin and indocyanine green. *Journal of hepatology*, 54:738–745, Apr. 2011.

- [13] M. D'Onofrio, R. De Robertis, A. Ruzzenente, W. Mantovani, G. Puntel, S. Crosara, S. Canestrini, A. Guglielmi, and R. P. Mucelli. Time-to-peak values can estimate hepatic functional reserve in patients undergoing surgical resection: a comparison between perfusion ct and indocyanine green retention test. *Journal of computer assisted tomography*, 38:733–741, 2014.
- [14] P. Fayzik, C.-G. Krenn, A. Baker, D. Lahner, G. Berlakovich, H. Steltzer, and H. Hetz. Comparison of invasive and noninvasive measurement of plasma disappearance rate of indocyanine green in patients undergoing liver transplantation: a prospective investigator-blinded study. *Liver transplantation : official publication of the American Association for the Study of Liver Diseases and the International Liver Transplantation Society*, 10:1060–1064, Aug. 2004.
- [15] W. D. Figg, G. E. Dukes, H. R. Lesesne, S. W. Carson, S. S. Songer, J. F. Pritchard, D. J. Hermann, J. R. Powell, and L. J. Hak. Comparison of quantitative methods to assess hepatic function: Pugh's classification, indocyanine green, antipyrine, and dextromethorphan. *Pharmacotherapy*, 15:693–700, 1995.
- [16] A. Gadano, A. Hadengue, F. Vachiery, R. Moreau, P. Sogni, T. Soupison, S. Yang, S. Cailmail, and D. Lebrec. Relationship between hepatic blood flow, liver tests, haemodynamic values and clinical characteristics in patients with chronic liver disease. *Journal of gastroenterology and hepatology*, 12:167–171, Feb. 1997.
- [17] I. T. Gilmore, J. H. Marigold, and R. P. Thompson. Half-life time or clearance of indocyanine green in patients with liver disease. *Hepato-gastroenterology*, 29:55–57, Apr. 1982.
- [18] S. L. Grainger, P. W. Keeling, I. M. Brown, J. H. Marigold, and R. P. Thompson. Clearance and non-invasive determination of the hepatic extraction of indocyanine green in baboons and man. *Clinical science (London, England : 1979)*, 64:207–212, Feb. 1983.
- [19] U. Grundmann, M. Ziehmer, H. Raahimi, P. Altmayer, R. Larsen, and H. P. Büch. [effect of the volatile anesthetics halothane, enflurane and isoflurane on liver circulation in the human]. *Anästhesiologie, Intensivmedizin, Notfallmedizin, Schmerztherapie : AINS*, 27:406–413, Nov. 1992.
- [20] J. Grzegorzewski, J. Brandhorst, K. Green, D. Eleftheriadou, Y. Duport, F. Barthorscht, A. Köller, D. Y. J. Ke, S. De Angelis, and M. König. Pk-db: pharmacokinetics database for individualized and stratified computational modeling. *Nucleic acids research*, 49:D1358–D1364, Jan. 2021.
- [21] C. Hackl, H. J. Schlitt, P. Renner, and S. A. Lang. Liver surgery in cirrhosis and portal hypertension. *World journal of gastroenterology*, 22:2725–2735, Mar. 2016.
- [22] S. Haegele, S. Reiter, D. Wanek, F. Offensperger, D. Pereyra, S. Stremitzer, E. Fleischmann, C. Brostjan, T. Gruenberger, and P. Starlinger. Perioperative non-invasive indocyanine green-clearance testing to predict postoperative outcome after liver resection. *PloS one*, 11:e0165481, 2016.

- [23] N. Harimoto, T. Yoshizumi, Y. Fujimoto, T. Motomura, Y. Mano, T. Toshima, S. Itoh, N. Harada, T. Ikegami, H. Uchiyama, Y. Soejima, and Y. Maehara. Surgery for hepatocellular carcinoma in patients with child-pugh b cirrhosis: Hepatic resection versus living donor liver transplantation. *World journal of surgery*, 42:2606–2616, Aug. 2018.
- [24] A. W. Hemming, C. H. Scudamore, C. R. Shackleton, M. Pudek, and S. R. Erb. Indocyanine green clearance as a predictor of successful hepatic resection in cirrhotic patients. *American journal of surgery*, 163:515–518, May 1992.
- [25] C. Herold, R. Heinz, M. Radespiel-Tröger, H. T. Schneider, D. Schuppan, and E. G. Hahn. Quantitative testing of liver function in patients with cirrhosis due to chronic hepatitis c to assess disease severity. *Liver*, 21:26–30, Feb. 2001.
- [26] M. Hucka, F. T. Bergmann, C. Chaouiya, A. Dräger, S. Hoops, S. M. Keating, M. König, N. Le Novère, C. J. Myers, B. G. Olivier, et al. The systems biology markup language (sbml): Language specification for level 3 version 2 core release 2. *Journal of Integrative Bioinformatics*, 2019.
- [27] P. M. Huet and J. Lelorier. Effects of smoking and chronic hepatitis b on lidocaine and indocyanine green kinetics. *Clinical pharmacology and therapeutics*, 28:208–215, Aug. 1980.
- [28] P. M. Huet and J. P. Villeneuve. Determinants of drug disposition in patients with cirrhosis. *Hepatology (Baltimore, Md.)*, 3:913–918, 1983.
- [29] G. H. Kamimori, N. Sirisuth, D. J. Greenblatt, and N. D. Eddington. The influence of the menstrual cycle on triazolam and indocyanine green pharmacokinetics. *Journal of clinical pharmacology*, 40:739–744, July 2000.
- [30] K. Kamisaka, Y. Yatsuji, H. Yamada, and H. Kameda. The binding of indocyanine green and other organic anions to serum proteins in liver diseases. *Clinica chimica acta; international journal of clinical chemistry*, 53:255–264, June 1974.
- [31] I. L. Kanstrup and K. Winkler. Indocyanine green plasma clearance as a measure of changes in hepatic blood flow. *Clinical physiology (Oxford, England)*, 7:51–54, Feb. 1987.
- [32] S. Kawasaki, Y. Sugiyama, T. Iga, M. Hanano, T. Beppu, M. Sugiura, K. Sanjo, and Y. Idezuki. Hepatic clearances of antipyrine, indocyanine green, and galactose in normal subjects and in patients with chronic liver diseases. *Clinical pharmacology and therapeutics*, 44:217–224, Aug. 1988.
- [33] T. Kawasaki, F. Moriyasu, T. Kimura, H. Someda, Y. Fukuda, and K. Ozawa. Changes in portal blood flow consequent to partial hepatectomy: Doppler estimation. *Radiology*, 180:373–377, Aug. 1991.
- [34] S. M. Keating, D. Waltemath, M. König, F. Zhang, A. Dräger, C. Chaouiya, F. T. Bergmann, A. Finney, C. S. Gillespie, T. Helikar, S. Hoops, R. S. Malik-Sheriff, S. L. Moodie, I. I. Moraru, C. J. Myers, A. Naldi, B. G. Olivier, S. Sahle, J. C. Schaff, L. P. Smith, M. J. Swat, D. Thieffry,

- L. Watanabe, D. J. Wilkinson, M. L. Blinov, K. Begley, J. R. Faeder, H. F. Gómez, T. M. Hamm, Y. Inagaki, W. Liebermeister, A. L. Lister, D. Lucio, E. Mjolsness, C. J. Proctor, K. Raman, N. Rodriguez, C. A. Shaffer, B. E. Shapiro, J. Stelling, N. Swainston, N. Tanimura, J. Wagner, M. Meier-Schellersheim, H. M. Sauro, B. Palsson, H. Bolouri, H. Kitano, A. Funahashi, H. Hermjakob, J. C. Doyle, M. Hucka, and S. L. . C. members. Sbml level 3: an extensible format for the exchange and reuse of biological models. *Molecular systems biology*, 16:e9110, Aug. 2020.
- [35] S. Keiding, P. Ott, and L. Bass. Enhancement of unbound clearance of icg by plasma proteins, demonstrated in human subjects and interpreted without assumption of facilitating structures. *Journal of hepatology*, 19:327–344, Nov. 1993.
- [36] Y. Kin, Y. Nimura, N. Hayakawa, J. Kamiya, S. Kondo, M. Nagino, M. Miyachi, and M. Kanai. Doppler analysis of hepatic blood flow predicts liver dysfunction after major hepatectomy. *World journal of surgery*, 18:143–149, 1994.
- [37] P. M. Klockowski, M. E. Lener, M. A. Sirgo, and M. L. Rocci. Comparative evaluation of the effects of isradipine and diltiazem on antipyrine and indocyanine green clearances in elderly volunteers. *Clinical pharmacology and therapeutics*, 48:375–380, Oct. 1990.
- [38] M. König. matthiaskoenig/sbmlsim: 0.1.14 - sbml simulation made easy, Mar. 2021.
- [39] M. König. matthiaskoenig/sbmlutils: 0.4.12 - python utilities for sbml, Mar. 2021.
- [40] C. M. Leevy, C. L. Mendenhall, W. Lesko, and M. M. Howard. Estimation of hepatic blood flow with indocyanine green. *The Journal of clinical investigation*, 41:1169–1179, May 1962.
- [41] C. M. Leevy, F. Smith, J. Longueville, G. Paumgartner, and M. M. Howard. Indocyanine green clearance as a test for hepatic function. evaluation by dichromatic ear densitometry. *JAMA*, 200:236–240, Apr. 1967.
- [42] E. Levesque, E. Hoti, D. Azoulay, R. Adam, D. Samuel, D. Castaing, and F. Saliba. Non-invasive icg-clearance: a useful tool for the management of hepatic artery thrombosis following liver transplantation. *Clinical transplantation*, 25:297–301, 2011.
- [43] E. Levesque, E. Martin, D. Dudau, C. Lim, G. Dhonneur, and D. Azoulay. Current use and perspective of indocyanine green clearance in liver diseases. *Anaesthesia, critical care & pain medicine*, 35:49–57, Feb. 2016.
- [44] J. F. Martin, M. Mikulecky, T. F. Blaschke, J. G. Waggoner, J. Vergalla, and P. D. Berk. Differences between the plasma indocyanine green disappearance rates of normal men and women. *Proceedings of the Society for Experimental Biology and Medicine. Society for Experimental Biology and Medicine (New York, N.Y.)*, 150:612–617, Dec. 1975.

- [45] J. F. Martin, J. M. Vierling, A. W. Wolkoff, B. F. Scharschmidt, J. Vergalla, J. G. Waggoner, and P. D. Berk. Abnormal hepatic transport of indocyanine green in gilbert's syndrome. *Gastroenterology*, 70:385–391, Mar. 1976.
- [46] D. K. Meijer, B. Weert, and G. A. Vermeer. Pharmacokinetics of biliary excretion in man. vi. indocyanine green. *European journal of clinical pharmacology*, 35:295–303, 1988.
- [47] S. Mukherjee, M. A. M. Rogers, and B. Buniak. Comparison of indocyanine green clearance with child's-pugh score and hepatic histology: a multivariate analysis. *Hepato-gastroenterology*, 53:120–123, 2006.
- [48] S. Møller, J. Hillingsø, E. Christensen, and J. H. Henriksen. Arterial hypoxaemia in cirrhosis: fact or fiction? *Gut*, 42:868–874, June 1998.
- [49] S. Møller, E. la Cour Sibbesen, J. L. Madsen, and F. Bendtsen. Indocyanine green retention test in cirrhosis and portal hypertension: Accuracy and relation to severity of disease. *Journal of gastroenterology and hepatology*, 34:1093–1099, June 2019.
- [50] C. U. Niemann, T. K. Henthorn, T. C. Krejcie, C. A. Shanks, C. Enders-Klein, and M. J. Avram. Indocyanine green kinetics characterize blood volume and flow distribution and their alteration by propranolol. *Clinical pharmacology and therapeutics*, 67:342–350, Apr. 2000.
- [51] T. Nonami, A. Nakao, T. Kurokawa, H. Inagaki, Y. Matsushita, J. Sakamoto, and H. Takagi. Blood loss and icg clearance as best prognostic markers of post-hepatectomy liver failure. *Hepato-gastroenterology*, 46:1669–1672, 1999.
- [52] S. Ohwada, S. Kawate, K. Hamada, T. Yamada, Y. Sunose, H. Tsutsumi, K. Tago, and T. Okabe. Perioperative real-time monitoring of indocyanine green clearance by pulse spectrophotometry predicts remnant liver functional reserve in resection of hepatocellular carcinoma. *The British journal of surgery*, 93:339–346, Mar. 2006.
- [53] O. Okochi, T. Kaneko, H. Sugimoto, S. Inoue, S. Takeda, and A. Nakao. Icg pulse spectrophotometry for perioperative liver function in hepatectomy. *The Journal of surgical research*, 103:109–113, Mar. 2002.
- [54] P. Ott. Hepatic elimination of indocyanine green with special reference to distribution kinetics and the influence of plasma protein binding. *Pharmacology & toxicology*, 83 Suppl 2:1–48, 1998.
- [55] G. Paumgartner, J. Huber, and G. Grabner. [kinetics of hepatic dye absorption for indocyanine green. influence of bilirubin and sodium glycocholate]. *Experientia*, 25:1219–1223, Nov. 1969.
- [56] Y. Peng, X. Qi, and X. Guo. Child-pugh versus meld score for the assessment of prognosis in liver cirrhosis: A systematic review and meta-analysis of observational studies. *Medicine*, 95:e2877, Feb. 2016.

- [57] M.-L. L. Pind, F. Bendtsen, T. Kallemose, and S. Møller. Indocyanine green retention test (icg-r15) as a noninvasive predictor of portal hypertension in patients with different severity of cirrhosis. *European journal of gastroenterology & hepatology*, 28:948–954, Aug. 2016.
- [58] R. Purcell, P. Kruger, and M. Jones. Indocyanine green elimination: a comparison of the limon and serial blood sampling methods. *ANZ journal of surgery*, 76:75–77, 2006.
- [59] L. B. Rowell, J. R. Blackmon, and R. A. Bruce. Indocyanine green clearance and estimated hepatic blood flow during mild to maximal exercise in upright man. *The Journal of clinical investigation*, 43:1677–1690, Aug. 1964.
- [60] S. G. Sakka. Assessment of liver perfusion and function by indocyanine green in the perioperative setting and in critically ill patients. *Journal of clinical monitoring and computing*, 32:787–796, Oct. 2018.
- [61] S. G. Sakka and N. van Hout. Relation between indocyanine green (icg) plasma disappearance rate and icg blood clearance in critically ill patients. *Intensive care medicine*, 32:766–769, May 2006.
- [62] Y. Seyama and N. Kokudo. Assessment of liver function for safe hepatic resection. *Hepatology research : the official journal of the Japan Society of Hepatology*, 39:107–116, Feb. 2009.
- [63] H. Shinohara, A. Tanaka, T. Kitai, N. Yanabu, T. Inomoto, S. Satoh, E. Hatano, Y. Yamaoka, and K. Hirao. Direct measurement of hepatic indocyanine green clearance with near-infrared spectroscopy: separate evaluation of uptake and removal. *Hepatology (Baltimore, Md.)*, 23:137–144, Jan. 1996.
- [64] L. P. Smith, M. Hucka, S. Hoops, A. Finney, M. Ginkel, C. J. Myers, I. Moraru, and W. Liebermeister. Sbml level 3 package: Hierarchical model composition, version 1 release 3. *Journal of integrative bioinformatics*, 12(2):603–659, 2015.
- [65] E. T. Somogyi, J.-M. Bouteiller, J. A. Glazier, M. König, J. K. Medley, M. H. Swat, and H. M. Sauro. libroadrunner: a high performance sbml simulation and analysis library. *Bioinformatics*, 31(20):3315–3321, 2015.
- [66] P. A. Soons, A. De Boer, A. F. Cohen, and D. D. Breimer. Assessment of hepatic blood flow in healthy subjects by continuous infusion of indocyanine green. *British journal of clinical pharmacology*, 32:697–704, Dec. 1991.
- [67] R. E. Stenson, R. T. Constantino, and D. C. Harrison. Interrelationships of hepatic blood flow, cardiac output, and blood levels of lidocaine in man. *Circulation*, 43:205–211, Feb. 1971.
- [68] M. Stockmann, J. F. Lock, B. Riecke, K. Heyne, P. Martus, M. Fricke, S. Lehmann, S. M. Niehues, M. Schwabe, A.-J. Lemke, and P. Neuhaus. Prediction of postoperative outcome after hepatectomy with a new bedside test for maximal liver function capacity. *Annals of surgery*, 250:119–125, July 2009.

- [69] Y. Sunagawa, S. Yamada, Y. Kato, F. Sonohara, H. Takami, Y. Inokawa, M. Hayashi, G. Nakayama, M. Koike, and Y. Kodera. Perioperative assessment of indocyanine green elimination rate accurately predicts postoperative liver failure in patients undergoing hepatectomy. *Journal of hepatobiliary-pancreatic sciences*, 28:86–94, Jan. 2021.
- [70] M. N. Thomas, E. Weninger, M. Angele, F. Bösch, S. Pratschke, J. Andrássy, M. Rentsch, M. Stangl, W. Hartwig, J. Werner, and M. Guba. Intraoperative simulation of remnant liver function during anatomic liver resection with indocyanine green clearance (limon) measurements. *HPB : the official journal of the International Hepato Pancreato Biliary Association*, 17:471–476, June 2015.
- [71] E. A. Tschoatzis, J. Bosch, and A. K. Burroughs. Liver cirrhosis. *Lancet (London, England)*, 383:1749–1761, May 2014.
- [72] M. Vaubourdolle, V. Gufflet, O. Chazouillères, J. Giboudeau, and R. Poupon. Indocyanine green-sulfobromophthalein pharmacokinetics for diagnosing primary biliary cirrhosis and assessing histological severity. *Clinical chemistry*, 37:1688–1690, Oct. 1991.
- [73] P. Virtanen, R. Gommers, T. E. Oliphant, M. Haberland, T. Reddy, D. Cournapeau, E. Burovski, P. Peterson, W. Weckesser, J. Bright, S. J. van der Walt, M. Brett, J. Wilson, K. J. Millman, N. Mayorov, A. R. J. Nelson, E. Jones, R. Kern, E. Larson, C. J. Carey, İ. Polat, Y. Feng, E. W. Moore, J. VanderPlas, D. Laxalde, J. Perktold, R. Cimrman, I. Henriksen, E. A. Quintero, C. R. Harris, A. M. Archibald, A. H. Ribeiro, F. Pedregosa, P. van Mulbregt, and SciPy 1.0 Contributors. SciPy 1.0: Fundamental Algorithms for Scientific Computing in Python. *Nature Methods*, 17:261–272, 2020.
- [74] H. Wakabayashi, K. Ishimura, K. Izuishi, Y. Karasawa, and H. Maeta. Evaluation of liver function for hepatic resection for hepatocellular carcinoma in the liver with damaged parenchyma. *The Journal of surgical research*, 116:248–252, Feb. 2004.
- [75] H. O. Wheeler, W. I. Cranston, and J. I. Meltzer. Hepatic uptake and biliary excretion of indocyanine green in the dog. *Proceedings of the Society for Experimental Biology and Medicine. Society for Experimental Biology and Medicine (New York, N.Y.)*, 99:11–14, Oct. 1958.

Eigenständigkeitserklärung

Hiermit erkläre ich, dass ich die vorliegende Arbeit selbständig verfasst habe und sämtliche Quellen, einschließlich Internetquellen, die unverändert oder abgewandelt wiedergegeben werden, insbesondere Quellen für Texte, Grafiken, Tabellen und Bilder, als solche kenntlich gemacht habe. Ich versichere, dass ich die vorliegende Abschlussarbeit noch nicht für andere Prüfungen eingereicht habe. Mir ist bekannt, dass bei Verstößen gegen diese Grundsätze ein Verfahren wegen Täuschungsversuchs bzw. Täuschung gemäß der fachspezifischen Prüfungsordnung und/oder der Fächerübergreifenden Satzung zur Regelung von Zulassung, Studium und Prüfung der Humboldt-Universität zu Berlin (ZSP-HU) eingeleitet wird.

Ort, Datum, Unterschrift

Berlin, 02.04.2021 A. Kölker